Supporting Information

Alkyl-initiated ring opening polymerization of lactide by indium complexes supported by NCN pincer ligands

*Takeo Iwase,‡ Afagh Habibzadeh,‡ Chatura Goonesingh, Kudzanai Nyamayaro, Joseph Chang, Jason Wai-Lok Poon, Salik Hasan Rushdy, Justin Koh, Brian O. Patrick, and Parisa Mehrkhodavandi**

* mehr@chem.ubc.ca

Department of Chemistry, University of British Columbia, 2036 Main Mall, Vancouver, British Columbia, V6T 1Z1, Canada

‡These authors contributed equally.

Table of Contents

A. Experimental procedures

General Considerations. Unless otherwise indicated, all air- and/or water-sensitive reactions were carried out under dry nitrogen using either an MBraun glove box or standard Schlenk line techniques. NMR spectra were recorded on a Bruker Avance 300 MHz and 400 MHz spectrometers. ^{1}H NMR chemical shifts are reported in ppm versus residual protons in deuterated solvents as follows: δ 7.27 $CDCl_3$, δ 7.16 C_6D_6, δ 2.12 toluene-d_8. $^{13}C\{^{1}H\}$ NMR chemical shifts are reported in ppm versus residual ^{13}C in the solvent: δ 77.2 $CDCl_3$, δ 127.9 C_6D_6. Diffraction measurements for X-ray crystallography were made on a Bruker X8 APEX II diffraction and a Bruker APEX DUO diffraction with graphite monochromated Mo-Kα radiation. The structures were solved by direct methods and refined by full-matrix least-squares using the SHELXTL crystallographic software of Bruker-AXS. Unless specified, all non-hydrogens were refined with anisotropic displacement parameters, and all hydrogen atoms were constrained to geometrically calculated positions but were not refined. EA CHN analysis was performed using a Carlo Erba EA1108 elemental analyzer. The elemental composition of unknown samples was determined by using a calibration factor. The calibration factor was determined by analyzing a suitable certified organic standard (OAS) of a known elemental composition.

Polymer molecular weights were determined by triple detection size exclusion chromatography (SEC-LLS) using a Waters liquid chromatograph equipped with a Water 515 HPLC pump, Waters 717 plus autosampler, Waters Styragel columns (4.6 × 300 mm) HR5E, HR4 and HR2, Water 2410 differential refractometer, Wyatt tristar miniDAWN (laser light scattering detector) and a Wyatt ViscoStar viscometer. A flow rate of 0.5 mL min^{-1} was used and samples were dissolved in THF (2 mg mL^{-1}). Narrow molecular weight polystyrene standards were used for calibration purposes. Matrix-assisted laser desorption/ionization time-of-flight (MALDI-TOF) mass spectrometric analysis of isolated polymers was performed on a Bruker Autoflex MALDI-TOF equipped with a nitrogen laser (337 nm). The accelerating potential of the Bruker instrument was 19.5 kV. The polymer samples were dissolved in tetrahydrofuran (ca. 10 mg/mL). The concentration of a cationization agent, sodium trifluoroacetate, in tetrahydrofuran was 1 mM. The matrix used was 2,5-Dihydroxybenzoic acid (DHB) at the concentration of 60 mg/mL. A sample solution was prepared by mixing polymer, matrix, and cation in a mole ratio of 1:1000:10, respectively.

Materials. Solvents (THF, toluene, hexane and diethyl ether) were collected from a Solvent Purification System from Innovative Technology, Inc. whose columns were packed with activated alumina. Dichloromethane (DCM), $CDCl_3$, and C_6D_6 were dried over CaH_2, collected by vacuum distillation and degassed through at least three freeze-pump-thaw cycles. *Rac*-lactide (rac-LA) was recrystallized three times from dry toluene and dried under vacuum. Isobutylmagnesium chloride (2.0 M in Et_2O), neosilylmagnesium chloride (2.0 M in Et_2O) and 2,6-diisopropylaniline were purchased from Aldrich and used as received. *p*TsOH.H_2O, zinc

granules (ACS, 20 mesh), and *p*-tert-butylphenol were purchased from Alfa Aesar and used without further purification. Pyridine and nitric acid (68–70 %) were purchased from Fisher Scientific. Pyridine was dried and stored in a bottle containing 5 Å molecular sieves. Other starting materials were obtained from Sigma Aldrich and used without further purification, unless stated otherwise. In(*i*Bu)$_3$ and In(CH_2SiMe_3)$_3$ were synthesized according to a previously reported procedure.[1] 2-Bromo-1,3-bis(bromomethyl)benzene was synthesized according to a previously reported procedure.[2] Proligands L1-3 were synthesized by the modification of a previously reported procedure.[3, 4]

Synthesis of L1

In a 250 mL RBF, 4,4'-Dimethyldiphenylamine (3.00 g, 8.76 mmol) and 1-bromo-2,6-bis(bromomethyl)benzene (7.77 g, 39.4 mmol) were dissolved in toluene (100 mL) then heated to reflux for 24 h. The slurry was filtered and the filtration was concentrated *in vacuo* to obtain a light brown powder. The light brown powder was washed with ethanol (250 mL) then dried under vacuum to get **L1** as an off white powder (53%). ^{1}H NMR (300 MHz, 25 °C, C_6D_6) δ 7.44 (d, *J* = 7.7 Hz, 2H), 7.04 – 6.80 (m, 8H), 5.04 (s, 2H), 2.09 (s, 4H). Anal. Calcd for C36H35BrN2: C 75.12; H 6.13; N 4.87. Found: C 74.74; H 5.93; N 5.00

Synthesis of L2

In a 250 mL RBF, dicyclohexylamine (3.00 g, 8.76 mmol) and 1-bromo-2,6-bis(bromomethyl)benzene (7.14 g, 39.4 mol) were dissolved in toluene (100 mL) then heated to reflux for 48 h. The white slurry was filtered and the filtration was concentrated *in vacuo* to obtain a white powder. The white powder was recrystallized in acetone at -20 °C to obtain **L2** as white crystals (73%). ^{1}H NMR (300 MHz, 298, $CDCl_3$) δ 7.57 (d, *J* = 7.5 Hz, 1H), 3.80 (s, 2H), 2.59 (qt, *J* = 9.1, 5.3 Hz, 2H), 1.85 – 1.06 (m, 20H). Anal. Calcd for C32H51BrN2: C 70.69; H 9.46; N 5.15. Found: C 71.41; H 9.61; N 5.20

Synthesis of L3

A modified literature methodology was used for the synthesis of **L3**.[3] In a 50 mL RBF, 5-(tert-butyl)-2-iodoisophthalaldehyde (5.00 g, 15.8 mmol), 2,6-diisopropylaniline (5.89 g, 33.2 mmol), and *p*TsOH·H_2O (0.60 g, 3.16 mmol). Toluene (25 mL) was added to the mixture then a Dean-Stark apparatus was installed to remove water during reflux at 140 °C for 16 h. The resulting orange solution was cooled to room temperature until a yellow precipitate was obtained. The precipitate was filtered, then dissolved in THF to leave impurities behind, concentrated *in vacuo* and washed with cold acetone (3 × 20mL) until a yellow powder was obtained with 80% yield. ^{1}H NMR (300 MHz, 25 °C, $CDCl_3$) δ 8.58 (s, 2H), 8.42 (s, 2H), 7.30 – 7.20 (m, 1H), 7.20 – 7.07 (m, 1H), 3.02 (hept, *J* = 6.9 Hz, 2H), 1.57 (s, 1H), 1.24 (d, *J* = 6.9 Hz, 12H).

Synthesis of 1

In a 20 mL scintillation vial, **L1** (0.200 g, 0.350 mmol) was dissolved in THF (5 mL) then cooled to −78 °C. 1.6 M *n*BuLi (0.22 mL)was added dropwise at −78 °C then stirred for 30 min. A solution of $(i\text{Bu})_2$InCl (0.09 g, 0.35 mmol) in THF (1 mL) was cooled to −35 °C. The solution of **L1** and *n*BuLi was added dropwise to the solution of $(i\text{Bu})_2$InCl at −78 °C then stirred for 1 h before warming to room temperature. The mixture was stirred at room temperature for 16 h. The solution was concentrated *in vacuo*, then the residue was extracted with toluene (5 mL) then filtered to collect the filtrate. The filtrate was concentrated *in vacuo* then washed with hexane (3 × 5mL) then diethyl ether (3 × 5mL) to obtain **1** as a white powder (72 %). ^{1}H NMR (400 MHz, 25 °C, $CDCl_3$) δ 7.12 – 6.93 (m, 19H), 4.75 (s, 4H), 2.29 (s, 12H), 1.96 (s, J = 6.5 Hz, 2H), 0.86 (d, J = 6.5 Hz, 12H), 0.67 (d, J = 6.6 Hz, 4H). ^{13}C{^{1}H} NMR (101 MHz, 25 °C, $CDCl_3$) δ 160.45 (Ar C), 146.90 (Ar C), 145.03 (Ar C), 132.32 (Ar C), 129.39 (Ar C), 129.23 (Ar C), 126.80 (Ar C), 124.01 (Ar C), 122.07 (Ar C), 120.24 (Ar C), 62.65 (CH_2), 30.69 (In-CH_2), 27.81 (*i*Bu CH), 27.63 (*i*Bu CH), 20.36 (*p*-toluene CH_3). Anal. Calcd for C44H53InN2: C 72.92; H 7.37; N 3.87. Found: C 72.21; H 7.31; N 3.79

Synthesis of 2

In a 20 mL scintillation vial, **L2** (0.200 g, 0.370 mmol) was dissolved in THF (5 mL) then cooled to −78 °C. 1.6 M *n*BuLi (0.23 mL) was added dropwise at −78 °C then stirred for 30 min. A solution of $(i\text{Bu})_2$InCl (0.10 g, 0.38 mmol) in THF (1 mL) was cooled to −35 °C. The solution of **L2** and *n*BuLi was added dropwise to the solution of $(i\text{Bu})_2$InCl at −78 °C then stirred for 1 h before warming to room temperature. The mixture was stirred at room temperature for 16 h. The solution was concentrated *in vacuo*, then the residue was extracted with hexane (15 mL) then filtered to collect the filtrate. The filtrate was concentrated *in vacuo* until *ca.* 2 mL then stored at −35 °C to recrystallize. **2** was obtained as white solids upon two recrystallizations with hexane (46%). ^{1}H NMR (300 MHz, 25 °C, $CDCl_3$) δ 7.22 – 7.04 (m, 3H), 3.83 (s, 4H), 2.68 (q, J = 6.6 Hz, 4H), 2.05 (s, J = 6.5 Hz, 2H), 1.84-1.00 (m, 40H), 0.97 (d, J = 6.5 Hz, 12H), 0.75 (d, J = 6.8 Hz, 4H). ^{13}C{^{1}H} NMR (101 MHz, 25 °C, $CDCl_3$) δ 159.87 (Ar C), 147.69 (Ar C), 125.89 (Ar C), 123.44 (Ar C), 60.03 (CH_2), 56.72 (Cy CH), 31.84 (Cy CH_2), 30.02 (In-CH_2), 28.15 (*i*Bu CH), 27.76 (*i*Bu CH), 26.31 (Cy CH_2), 25.79 (Cy CH_2). Anal. Calcd for C40H69InN2: C 69.35; H 10.04; N 4.04. Found: C 69.28; H 10.09; N 3.95

Synthesis of 3

In a 20 mL scintillation vial, **L3** (0.200 g, 0.320 mmol) was dissolved in THF (5 mL) then cooled to −78 °C. 1.6 M *n*BuLi (0.20 mL) was added dropwise at −78 °C then stirred for 30 min. A solution of $(i\text{Bu})_2$InCl (0.09 g, 0.32mmol) in THF (1 mL) was cooled to −35 °C. The solution of **L3** and *n*BuLi was added dropwise to the solution of $(i\text{Bu})_2$InCl at −78 °C then stirred for 1 h before warming to room temperature. The mixture was stirred at room temperature for 16 h. The solution was concentrated *in vacuo*, then the residue was extracted with toluene (5 mL) then

filtered to collect the filtrate. The filtrate was concentrated *in vacuo* then washed with ACN (5 × 5 mL) to obtain **3** as a yellow white powder (60%). ^{1}H NMR (400 MHz, 25 °C, $CDCl_3$) δ 8.39 (s, 2H), 7.70 (s, 2H), 7.18 (s, 6H), 3.05 (s, *J* = 6.8 Hz, 4H), 1.78 (s, *J* = 6.7 Hz, 2H), 1.44 (s, 9H), 1.19 (d, *J* = 6.8 Hz, 24H), 0.68 (d, *J* = 6.6 Hz, 12H), 0.66 (d, *J* = 7 Hz, 4H). ^{13}C{^{1}H} NMR (101 MHz, 25 °C, $CDCl_3$) δ 168.59 (N=CH), 164.31 (Ar C), 151.03 (Ar C), 148.19 (Ar C), 142.42 (Ar C), 139.80 (Ar C), 131.70 (Ar C), 125.37 (Ar C), 123.58 (Ar C), 34.94 (*t*Bu C), 31.70 (In-CH2), 28.33 (*i*Bu CH), 28.01 (*i*Bu CH_3), 27.94 (*i*Pr CH), 27.80 (*i*Pr CH_3), 24.82 (*t*Bu CH_3). Anal. Calcd for C44H65InN2: C 71.72; H 8.89; N 3.80. Found: C 71.23; H 8.86; N 3.83

Synthesis of 4

In a 20 mL scintillation vial, **L2** (0.200 g, 0.370 mmol) was dissolved in THF (5 mL) then cooled to −78 °C. 1.6 M *n*BuLi (0.23 mL) was added dropwise at −78 °C then stirred for 30 min. A solution of $(CH_2SiMe_3)_2InCl$ (0.12 g, 0.38 mmol) in THF (1 mL) was cooled to −35 °C. The solution of **L2** and *n*BuLi was added dropwise to the solution of $(CH_2SiMe_3)_2InCl$ at −78 °C then stirred for 1 h before warming to room temperature. The mixture was stirred at room temperature for 16 h. The solution was concentrated *in vacuo*, then the residue was extracted with hexane (15 mL) then filtered to collect the filtrate. The filtrate was concentrated *in vacuo* until *ca.* 2 mL then stored in the freezer to recrystallize. **2** was obtained as a white solid (61%). ^{1}H NMR (400 MHz, 25 °C, $CDCl_3$) δ 7.17(d, J = 7.4 Hz, 2H), 7.11 (t, J = 7.6 Hz, 1H), 3.80 (s, 4H), 2.68 (t, J = 11.4 Hz, 4H), 1.9-0.82 (m, Cy-H, 44H), -0.02 (s, 18H), -0.39 (s, 2H. ^{13}C{^{1}H} NMR (101 MHz, 25 °C, $CDCl_3$) δ 147.64 (Ar C), 126.50 (Ar C), 124.14 (Ar C), 77.21, 60.41 (CH_2), 56.92 (Cy CH), 32.28 (Cy CH_2), 26.61 (Cy CH_2), 26.05 (Cy CH_2), 3.00 (**C**H_2(SiMe)$_3$, 2.49 (CH_2(Si**Me**)$_3$. Anal. Calcd for C40H73InN2Si2: C 63.80; H 9.77; N 3.72. Found: 63.37; H 9.68; N 3.93

Representative polymerization of rac-LA for initiators 1-3

A 20 mL scintillation vial was charged with a solution of **1** (5.0 mg, 0.007 mmol) in 0.5 mL of toluene. *Rac*-LA (199 mg, 1.38 mmol) was directly added to the vial. The mixture was stirred at 100 °C for the given hours. The resulting solution was cooled to room temperature then concentrated under vacuum for 3 h. The resulting residue was dissolved in DCM (3 mL) until homogenous then cold methanol was slowly added to the vial (0 °C, 15 mL). The polymer precipitated from the solution and was isolated by decantation of the supernatant. The isolated polymer was dried under high vacuum for at least 12 h prior to analysis.

Representative polymerization of rac-LA with for 5 + L1-3

A 20 mL scintillation vial was charged with a solution of **5** (5.0 mg, 0.007 mmol) and **L1** (10.9 mg, 0.007 mmol) in 0.5 mL of toluene. *Rac*-LA (544.9 mg, 1.38 mmol) was directly added to the vial. The mixture was stirred at 100 °C for the given hours. The resulting solution was cooled to

room temperature then concentrated under vacuum for 3 h. The resulting residue was dissolved in DCM (3 mL) until homogenous then cold methanol was slowly added to the vial (0 °C, 15 mL). The polymer precipitated from the solution and was isolated by decantation of the supernatant. The isolated polymer was dried under high vacuum for at least 12 h prior to analysis.

Representative oligomerization of rac-LA for 1-4 (MALDI-TOF analysis)

A 20 mL scintillation vial was charged with a solution of **1** (5.0 mg, 0.007 mmol) in 0.5 mL of toluene. *Rac*-LA (19.9 mg, 0.14 mmol) was directly added to the vial. The mixture was stirred at 100 °C for 4 hours. The resulting solution was cooled to room temperature then concentrated under vacuum for 3 h. The resulting residue was dissolved in DCM (0.3 mL) until homogenous then cold pentane was slowly added to the vial (0 °C, 15 mL). The polymer precipitated from the solution and was isolated by decantation of the supernatant. The isolated polymer was dried under high vacuum for at least 12 h prior to analysis.

Representative oligomerization of rac-LA for 1-4 (NMR analysis)

A 20 mL scintillation vial was charged with a solution of **1** (5.0 mg, 0.007 mmol) in 0.5 mL of toluene. *Rac*-LA (5.0 mg, 0.034 mmol) was directly added to the vial. The mixture was stirred at 100 °C for 4 hours. The resulting solution was cooled to room temperature then concentrated under vacuum for 3 h. The resulting residue was dissolved in DCM (0.3 mL) until homogenous then cold pentane was slowly added to the vial (0 °C, 15 mL). The polymer precipitated from the solution and was isolated by decantation of the supernatant. The isolated polymer was dried under high vacuum for at least 12 h prior to analysis.

Sample preparation for *in situ* ^{1}H NMR studies

A 1 mL scintillation vial was charged with **1** (5.0 mg, 0.007 mmol) and was quantitatively transferred with 0.4 mL of toluene-d_8 to a J. Young tube with *rac*-LA (5.0 mg, 0.034 mmol) and sealed. The ^{1}H NMR spectrum of the reaction mixture was obtained at regular intervals at 100 ^{o}C.

B. Characterization of proligands and indium complexes in solution

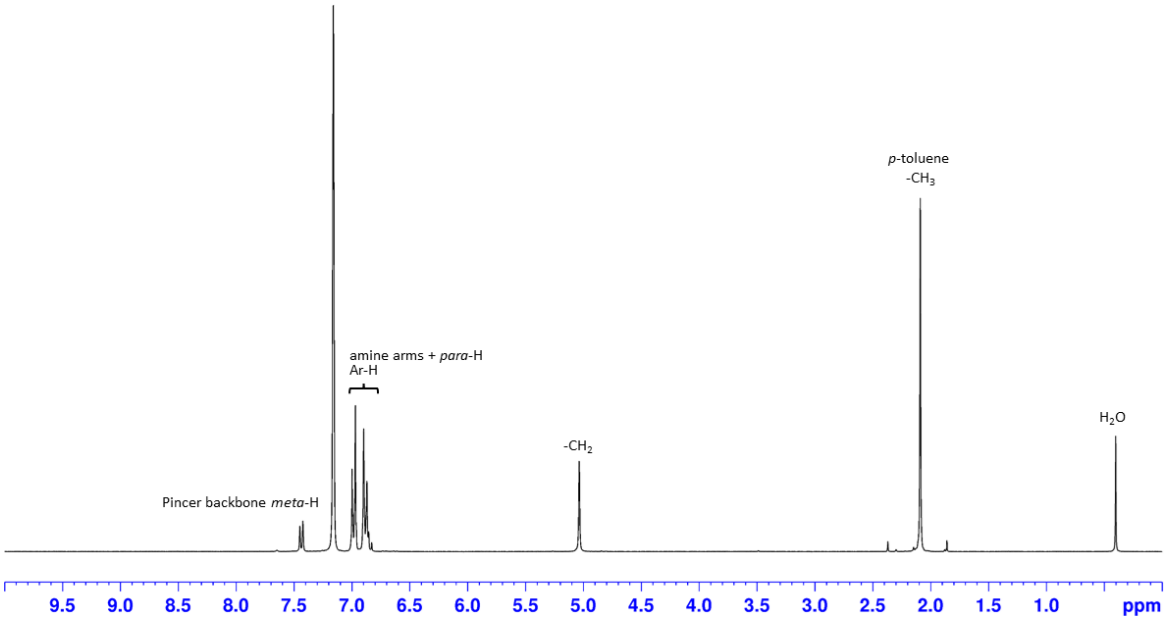

Figure S1 ^{1}H NMR spectrum (300 MHz, C_6D_6, 25 °C) of **L1**

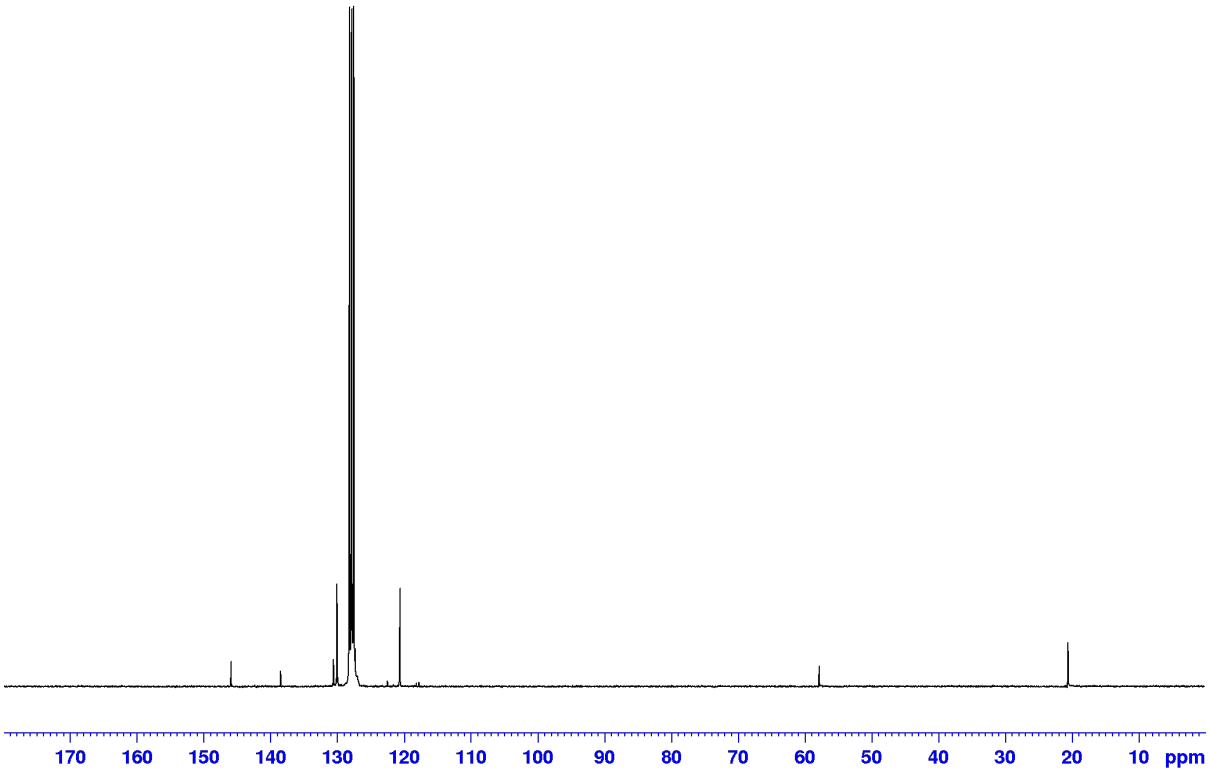

Figure S2 $^{13}C\{^{1}H\}$ NMR spectrum (75 MHz, C_6D_6, 25 °C) of **L1**

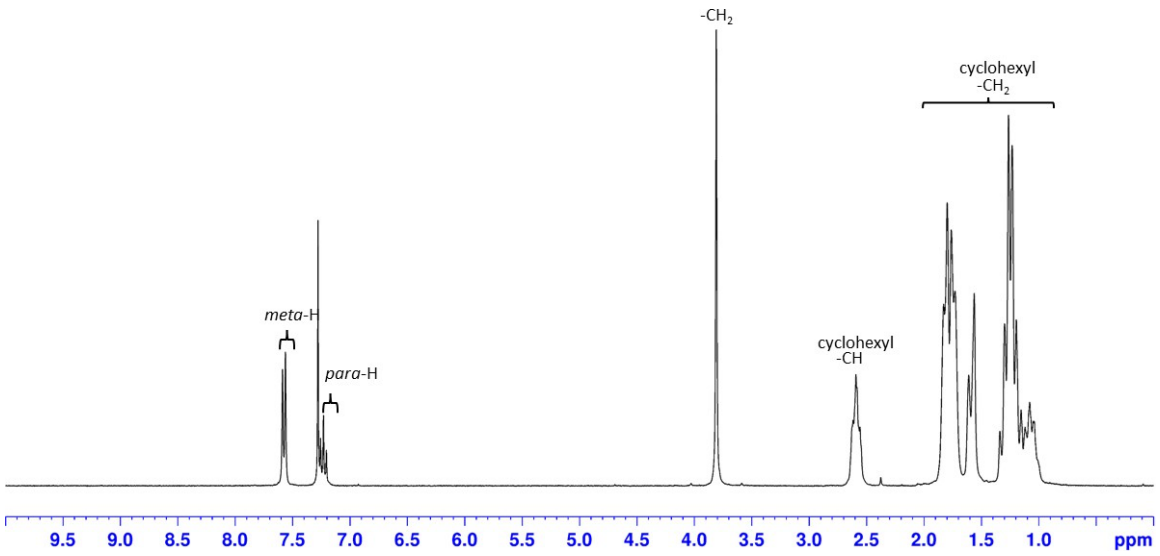

Figure S3 ^{1}H NMR spectrum (300 MHz, $CDCl_3$, 25 °C) of **L2**

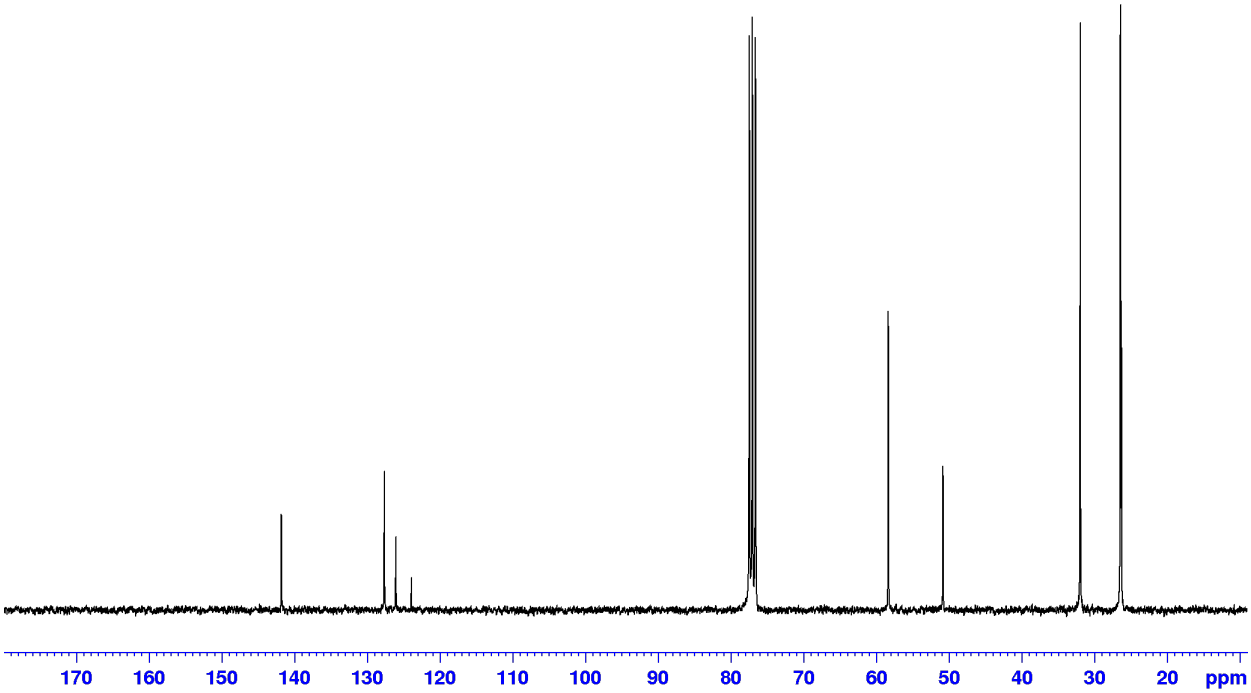

Figure S4 $^{13}C\{^{1}H\}$ NMR spectrum (75 MHz, CDCl, 25 °C) of **L2**

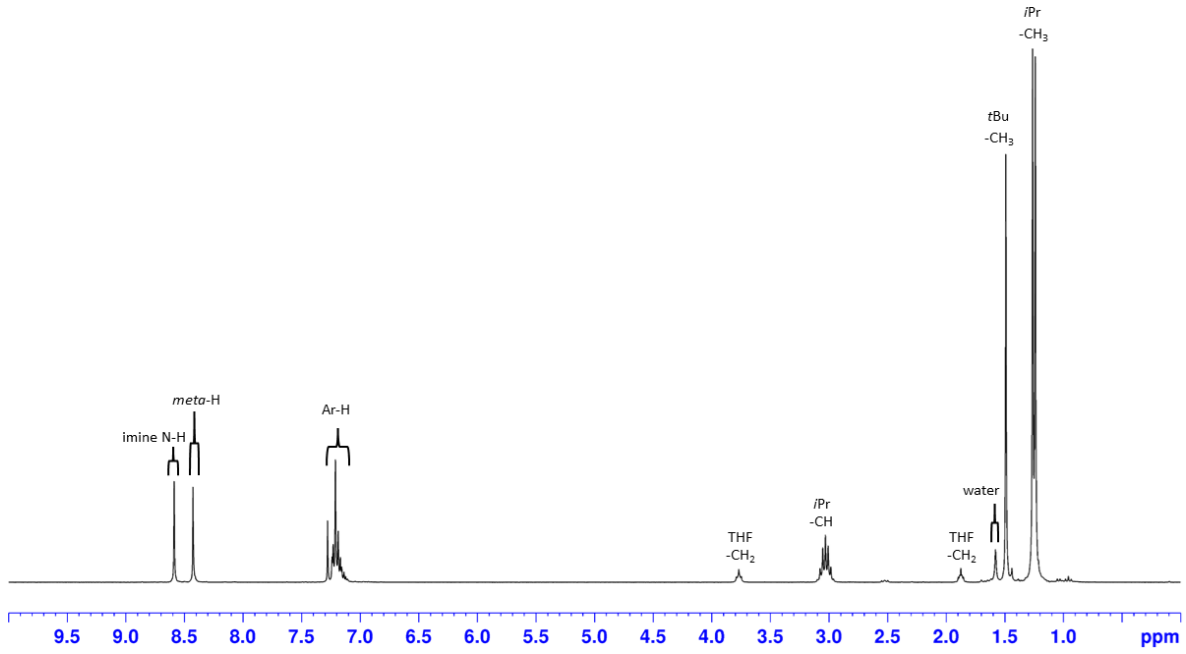

Figure S5 ^{1}H NMR spectrum (300 MHz, $CDCl_3$, 25 °C) of **L3**

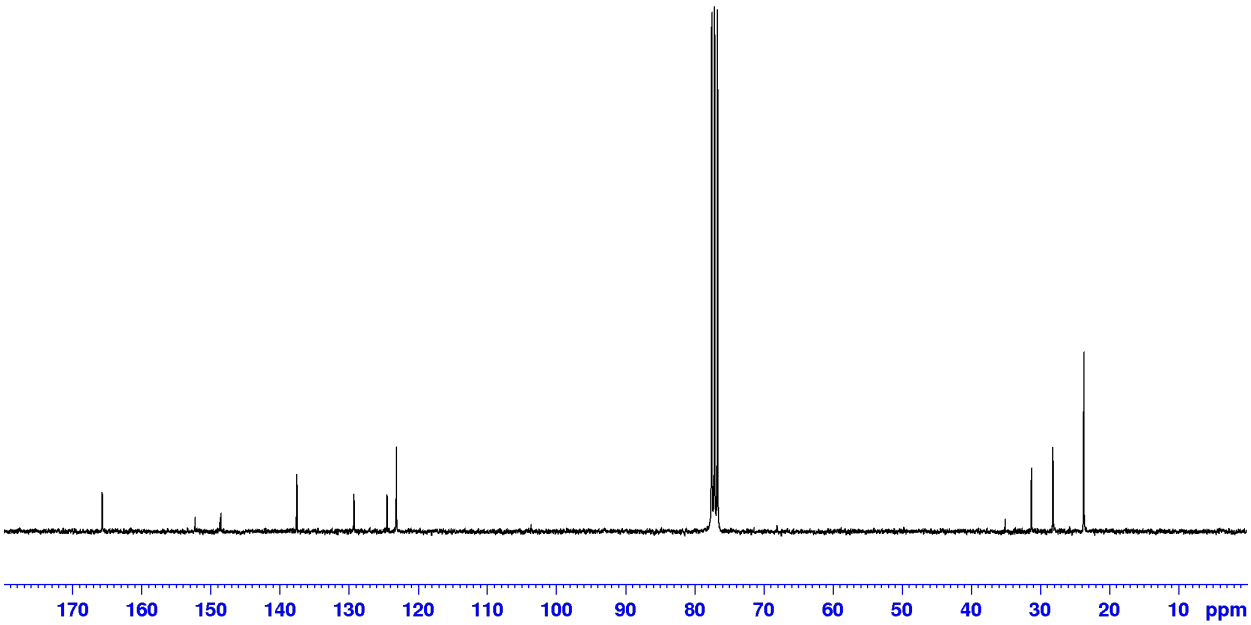

Figure S6 $^{13}C\{^{1}H\}$ NMR spectrum (75 MHz, $CDCl_3$, 25 °C) of **L3**

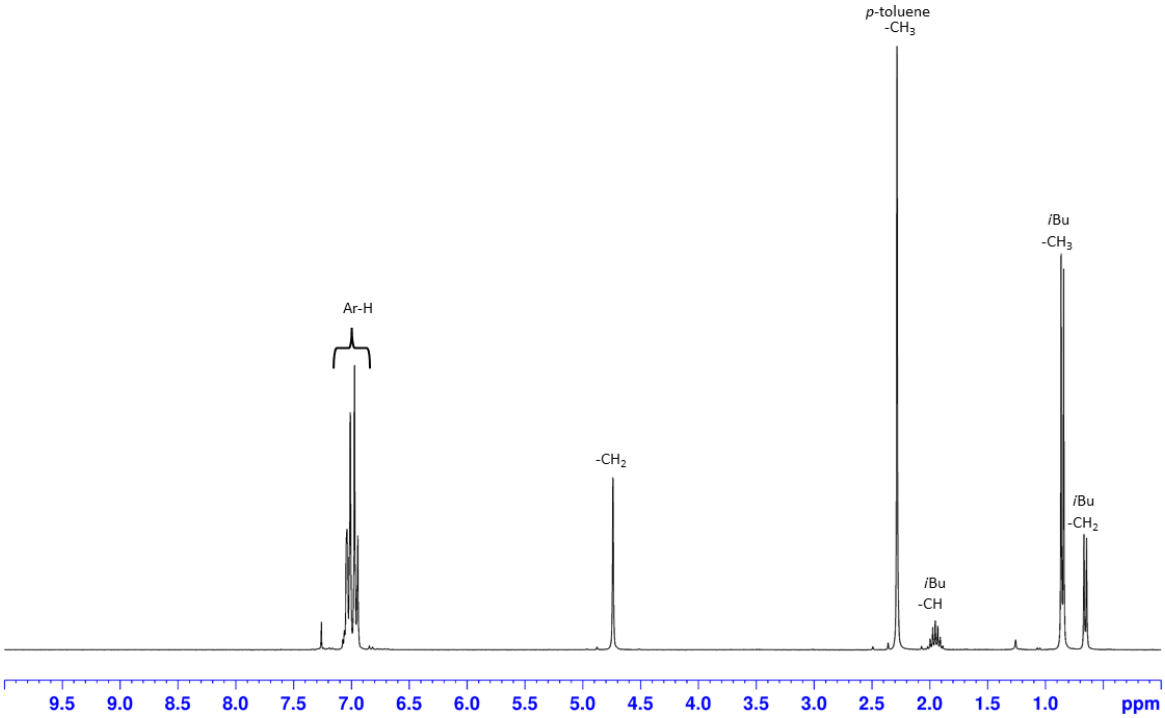

Figure S7 ^{1}H NMR spectrum (400 MHz, $CDCl_3$, 25 °C) of **1**

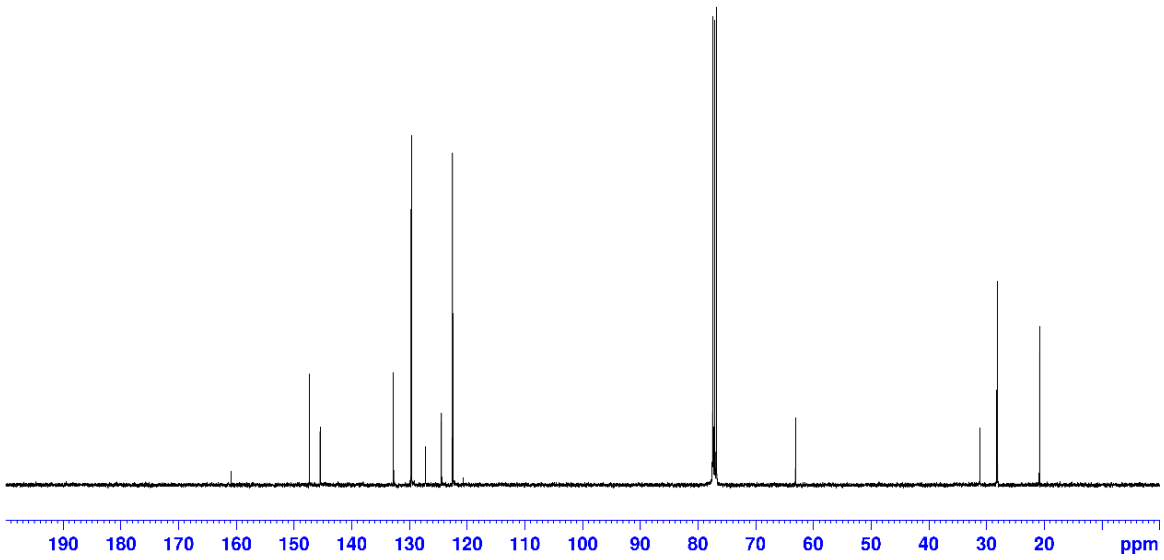

Figure S8 $^{13}C\{^{1}H\}$ NMR spectrum (101 MHz, $CDCl_3$, 25 °C) of **1**

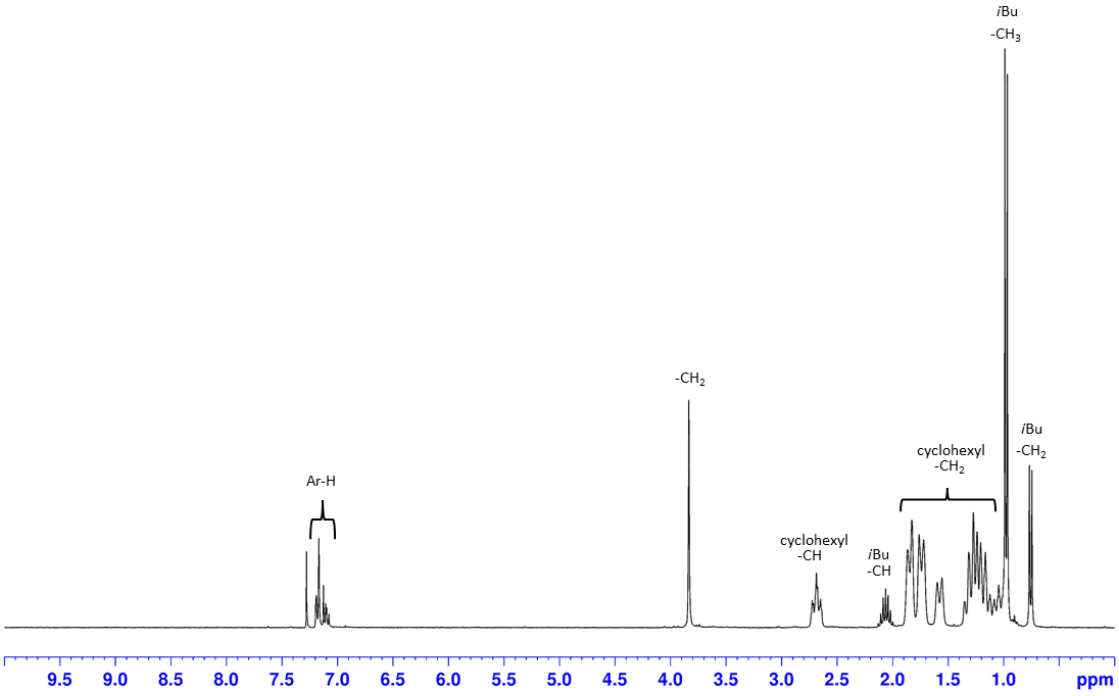

Figure S9 ^{1}H NMR spectrum (400 MHz, $CDCl_3$, 25 °C) of **2**

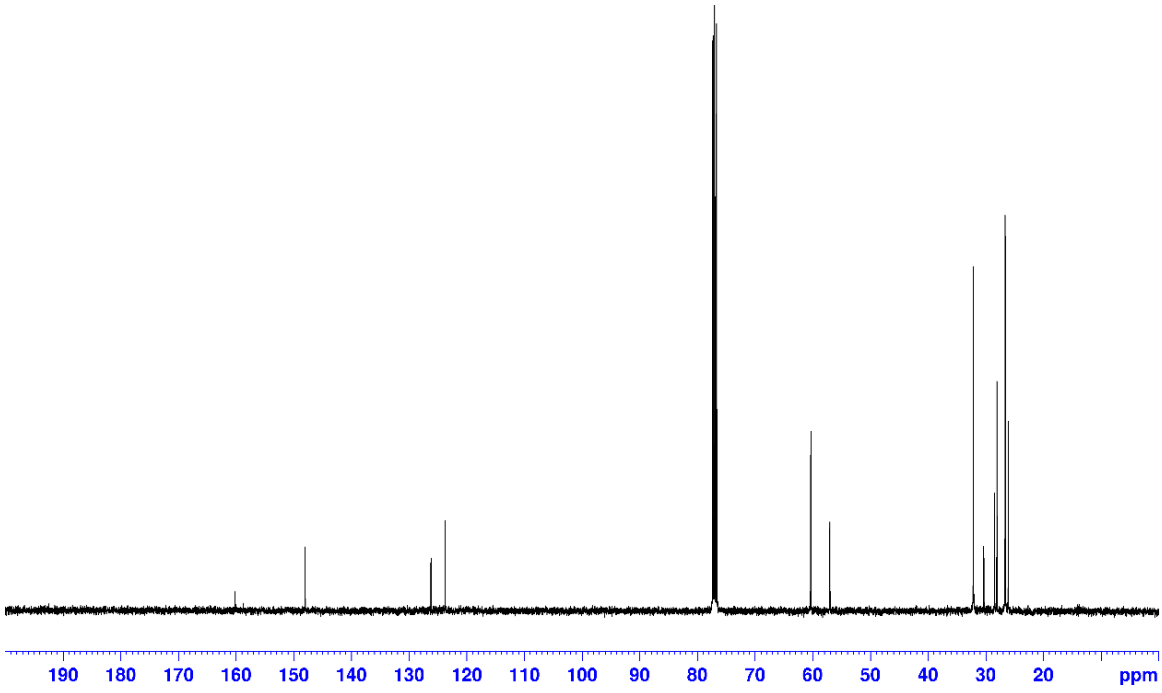

Figure S10 $^{13}C\{^{1}H\}$ NMR spectrum (101 MHz, $CDCl_3$, 25 °C) of **2**

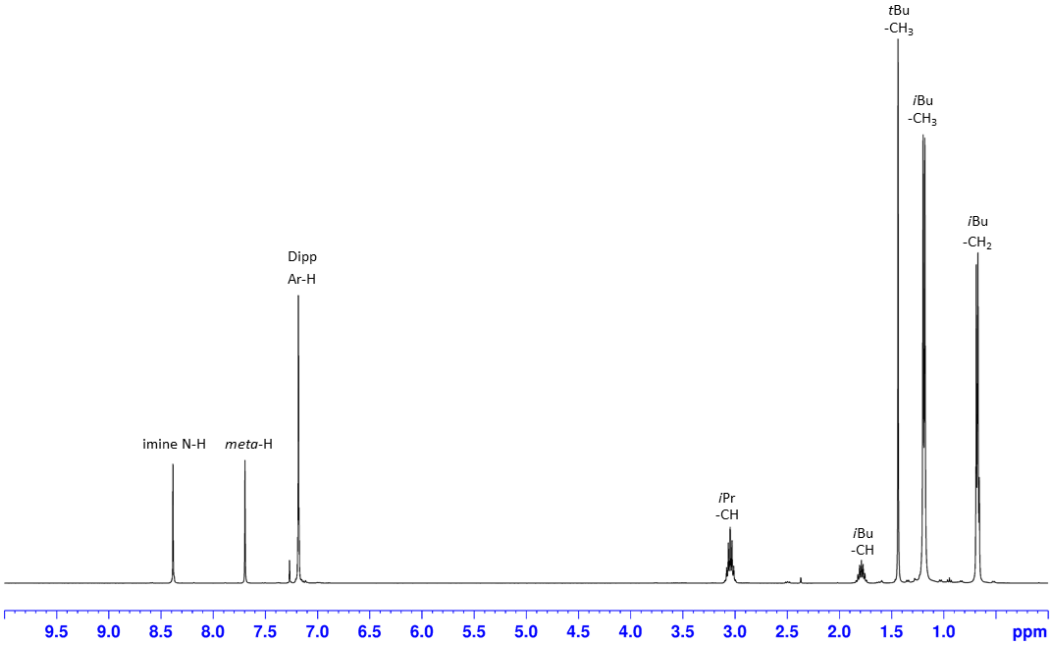

Figure S11 ^{1}H NMR spectrum (400 MHz, $CDCl_3$, 25 °C) of **3**

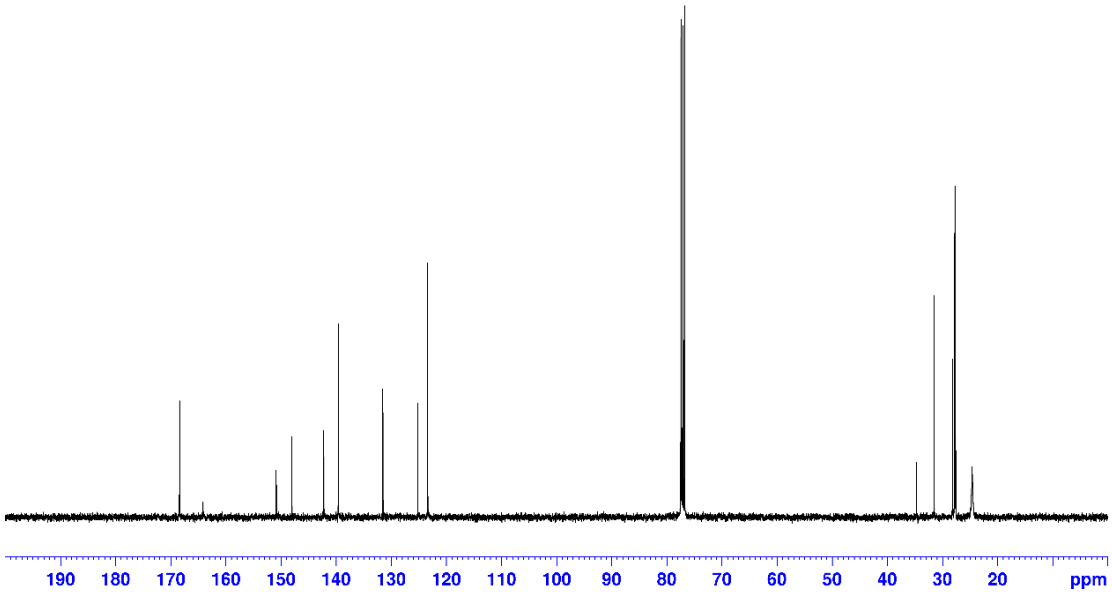

Figure S12 $^{13}C\{^{1}H\}$ NMR spectrum (101 MHz, $CDCl_3$, 25 °C) of **3**

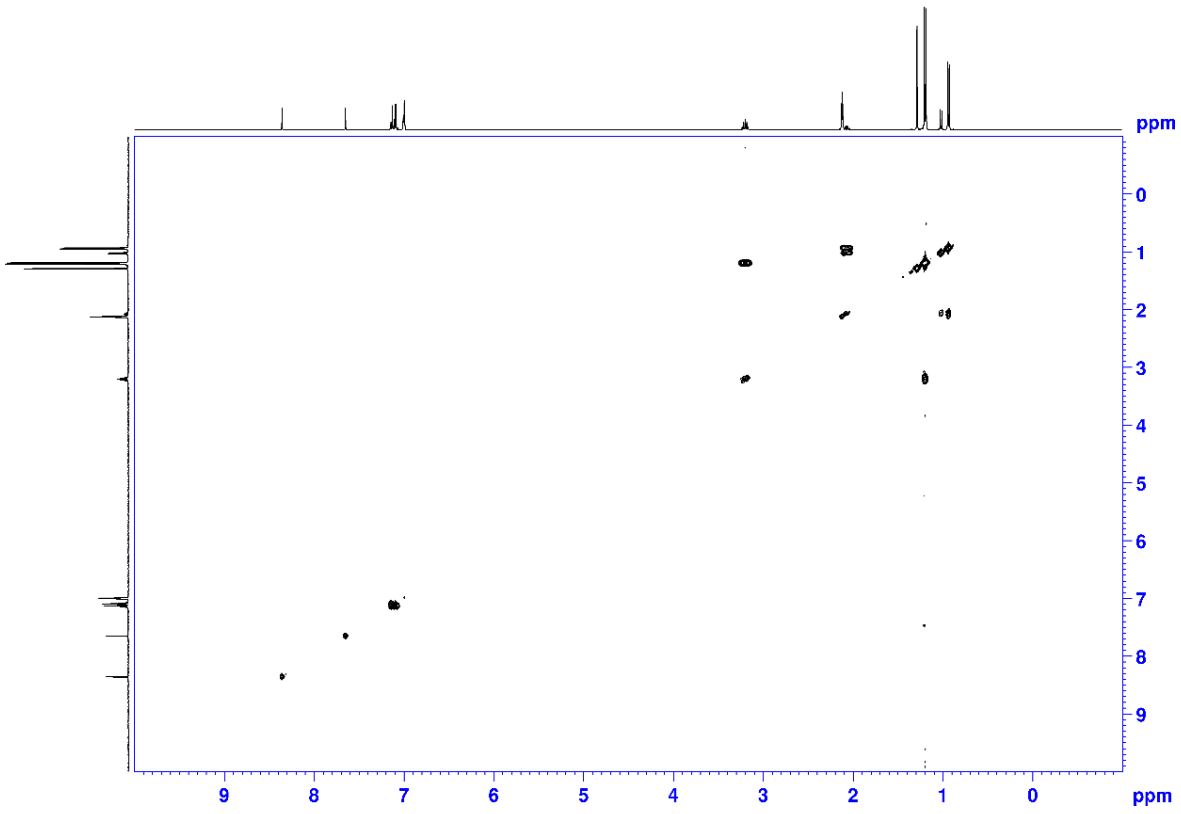

Figure S13 ^{1}H-^{1}H Correlation spectroscopy (COSY) NMR spectrum (400 MHz, toluene-d_8, 100 °C) of **3**

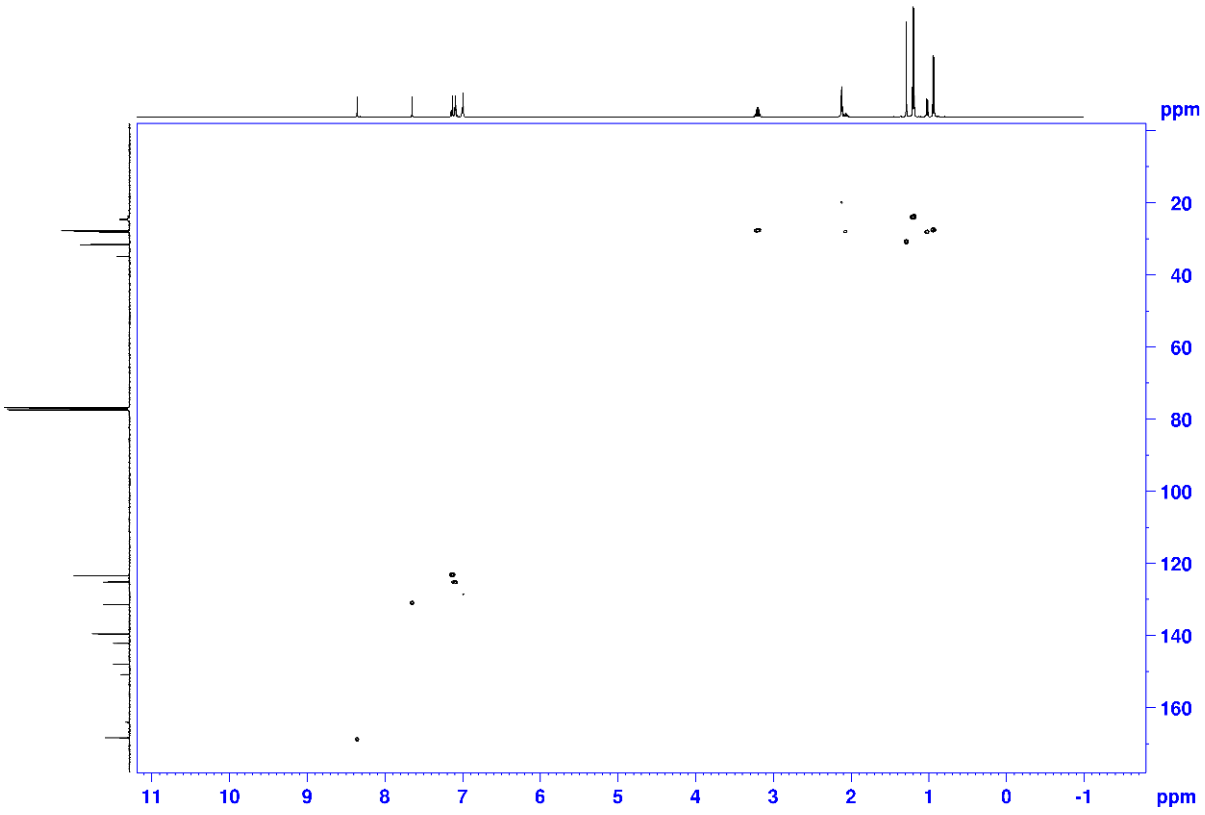

Figure S14 ^{1}H-^{13}C Heteronuclear single quantum correlation (HSQC) NMR spectrum (400 MHz, toluene-d_8, 100 °C) of **3**

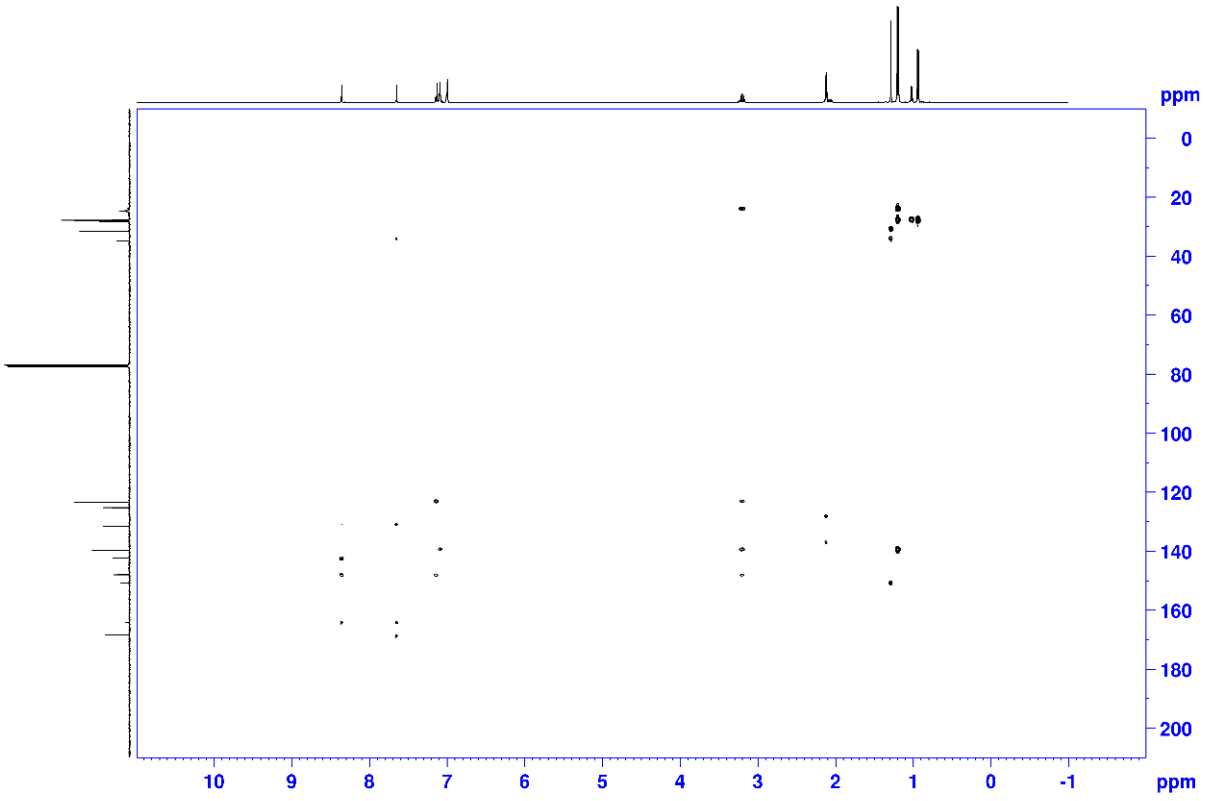

Figure S15 ^{1}H-^{13}C Heteronuclear multiple bond correlation (HMBC) NMR spectrum (400 MHz, toluene-d_8, 100 °C) of **3**

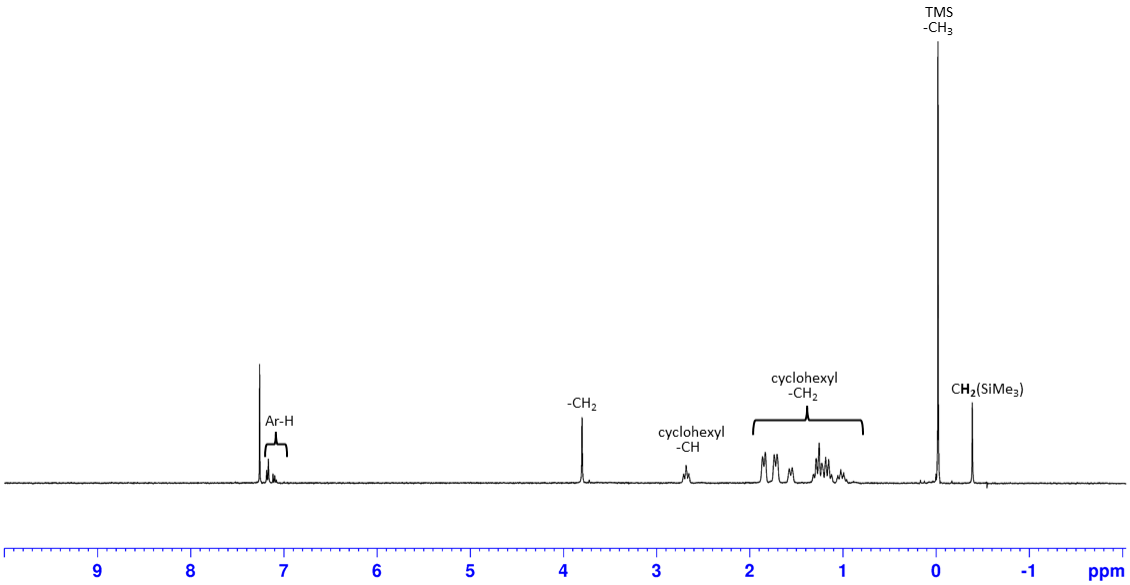

Figure S16 ^{1}H NMR spectrum (400 MHz, $CDCl_3$, 25 °C) of **4**

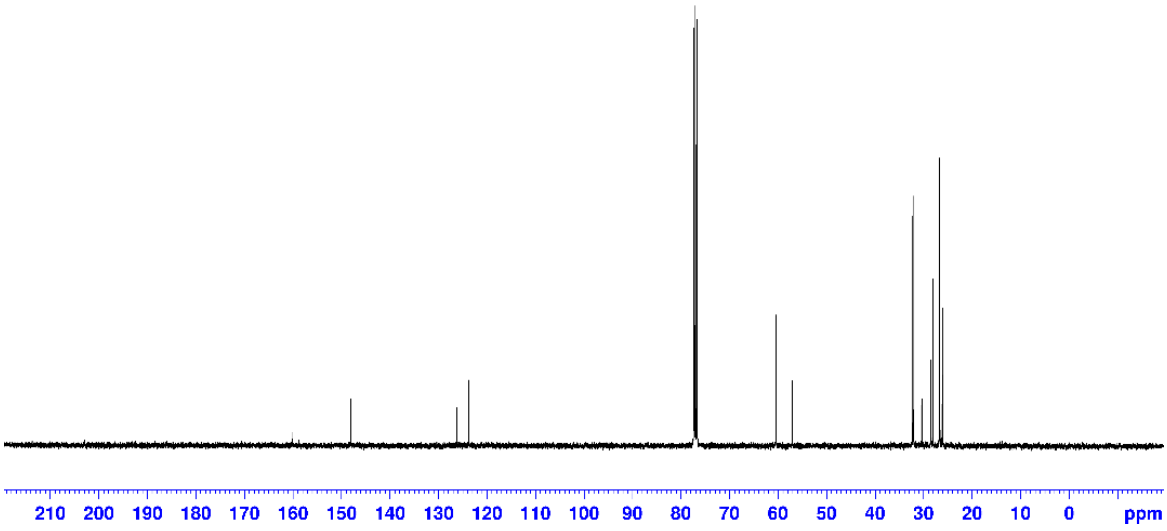

Figure S17 $^{13}C\{^{1}H\}$ NMR spectrum (101 MHz, $CDCl_3$, 25 °C) of **4**

C. Characterization of indium complexes in the solid state

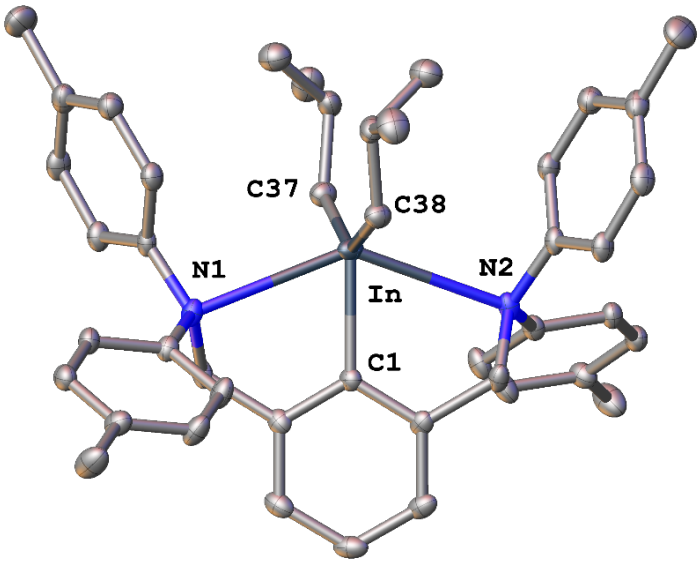

Figure S18 Molecular structure of depicted with thermal ellipsoids at 50% probability and H atoms omitted for clarity.

Table S1 Selected bond lengths and bond angles for complex **1**.

Selected bond length (Å) and angles (°) for complex **1**.				
Bond Lengths	In-N1	2.8923(12)	In-C37	2.1777(15)
	In-N2	2.8923(12)	In-C38	2.1777(15)
	In-C1	2.1761(19)		
Bond Angles	N1-In-N2	139.45 (5)	N1-In-C37	97.34 (5)
	C37-In-C38	139.70(8)	N2-In-C38	97.34 (5)
	N1-In-C1	69.72(2)	C1-In-C37	110.15(4)

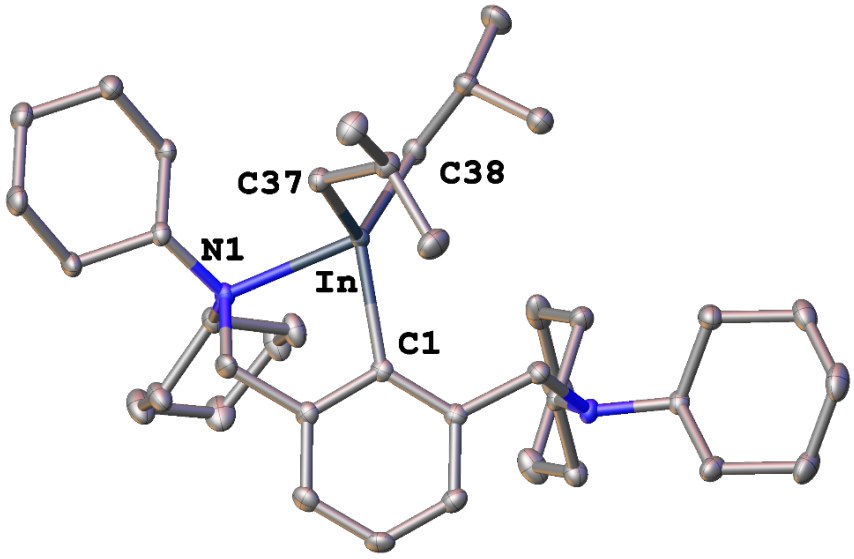

Figure S19 Molecular structure of **2** depicted with thermal ellipsoids at 50% probability and H atoms and minor disorders omitted for clarity.

Table S2 Selected bond lengths and bond angles for complex **2**.

Selected bond length (Å) and angles (°) for complex **2**.				
Bond Lengths	In-N1	2.4673 (13)	In-C37	2.2040 (16)
	In-C1	2.1792 (16)	In-C38	2.1857 (16)
Bond Angles	C37-In-C38	113.89 (6)	C1-In-C37	127.47 (6)
	N1-In-C1	78.39 (5)	C1-In-C38	113.89 (6)

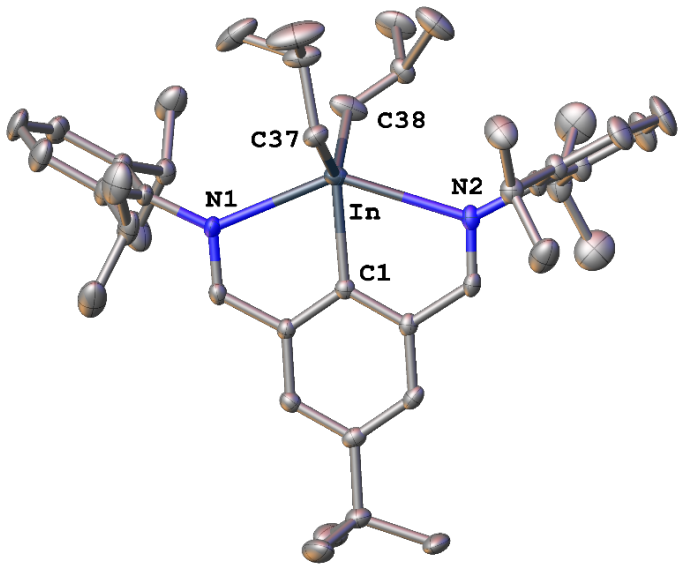

Figure S20 Molecular structure of **3** depicted with thermal ellipsoids at 50% probability and H atoms and minor disorders omitted for clarity.

Table S3 Selected bond lengths and bond angles for complex **3**.

Selected bond length (Å) and angles (°) for complex **3**.				
Bond Lengths	In-N1	2.6055(15)	In-C37	2.1832(19)
	In-N2	2.7026 (15)	In-C38	2.186(2)
	In-C1	2.1760(18)		
Bond Angles	N1-In-N2	140.19 (5)	N1-In-C37	99.83(6)
	C37-In-C38	123.09(8)	N2-In-C38	98.87 (8)
	N1-In-C1	70.72(6)	C1-In-C37	119.52(7)

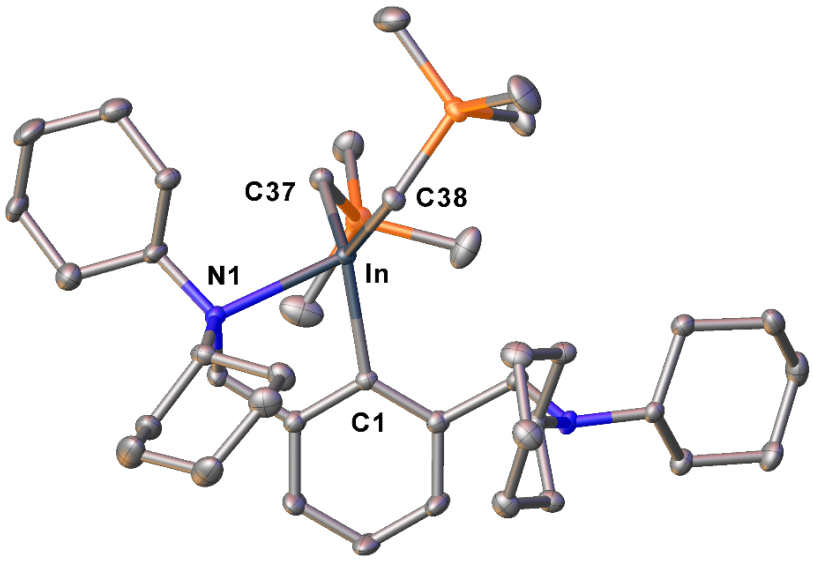

Figure S21 Molecular structure of **4** depicted with thermal ellipsoids at 50% probability and H atoms and minor disorders omitted for clarity.

Table S4 Selected bond lengths and bond angles for complex **4**.

Selected bond length (Å) and angles (°) for complex **2**.				
Bond Lengths	In-N1	2.4716 (15)	In1-C37	2.2056 (19)
	In-C1	2.1710 (18)	In1-C38	2.1783 (19)
Bond Angles	C37-In-C38	117.87 (7)	C1-In-C37	115.19 (7)
	N1-In-C1	77.66 (6)	C1-In-C38	121.97 (7)

Table S5 Selective crystal data

	Complex 1	**Complex 2**	**Complex 3**
Identification code	pm318	pm324	pm317
Empirical formula	$C_{44}H_{53}InN_2$	$C_{40}H_{69}InN_2$	$C_{45.11}H_{66.33}InN_{2.56}$
Formula weight	724.70	692.79	759.25
Temperature/K	296.15	273.15	273.15
Crystal system	monoclinic	monoclinic	monoclinic
Space group	C2/c	$P2_1/c$	$P2_1/n$
a/Å	20.5531(13)	10.2982(3)	17.9757(5)
b/Å	18.9727(13)	20.2667(5)	21.0050(6)
c/Å	11.3073(7)	18.1203(5)	23.9868(7)
α/°	90	90	90
β/°	122.928(2)	96.9660(10)	104.1180(10)
γ/°	90	90	90
Volume/$Å^3$	3700.9(4)	3753.98(18)	8783.4(4)
Z	4	4	8
$\rho_{calc}g/cm^3$	1.301	1.226	1.148
μ/mm^{-1}	0.671	0.658	0.568
F(000)	1520.0	1488	3231.0
Crystal size/mm^3	0.2 × 0.1 × 0.1	0.27 × 0.15 × 0.07	0.2 × 0.1 × 0.09
Radiation	MoKα (λ = 0.71073)	MoKα (λ = 0.71073)	MoKα (λ = 0.71073)
2Θ range for data collection/°	3.19 to 61.216	3.028 to 61.176	2.554 to 61.152
Index ranges	-27 ≤ h ≤ 29, -26 ≤ k ≤ 27, -16 ≤ l ≤ 15	-14 ≤ h ≤ 14, -28 ≤ k ≤ 28, -14 ≤ l ≤ 25	-22 ≤ h ≤ 25, -29 ≤ k ≤ 30, -34 l ≤ 34
Reflections collected	19380	83007	159046
Independent reflections	5666 [R_{int} = 0.0223, R_{sigma} = 0.0220]	11542 [Rint = 0.0392, Rsigma = 0.0289]	26929 [R_{int} = 0.0486, R_{sigma} = 0.0395]
Data/restraints/parameters	5666/0/218	11542/0/392	26929/32/1036
Goodness-of-fit on F^2	1.087	1.021	1.046
Final R indexes [I>=2σ (I)]	R_1 = 0.0270, wR_2 = 0.0702	R_1 = 0.0258, wR_2 = 0.0564	R_1 = 0.0395, wR_2 = 0.0720
Final R indexes [all data]	R_1 = 0.0313, wR_2 = 0.0730	R_1 = 0.0372, wR_2 = 0.0605	R_1 = 0.0631, wR_2 = 0.0801
Largest diff. peak/hole / e $Å^{-3}$	0.99/-0.43	0.66/-0.55	0.55/-0.75

Table S5 Selective crystal data continued

	Complex 4
Identification code	pm326
Empirical formula	$C_{40}H_{73}N_2Si_2In$
Formula weight	753
Temperature/K	296.15
Crystal system	monoclinic
Space group	$P2_1/n$
a/Å	9.4655(5)
b/Å	23.9882(13)
c/Å	18.4803(10)
α/°	90
β/°	91.112(2)
γ/°	90
Volume/Å^3	4195.4(4)
Z	4
ρ_{calc}g/cm^3	1.192
μ/mm^{-1}	0.648
F(000)	1616
Crystal size/mm^3	0.32 × 0.07 × 0.03
Radiation	MoKα (λ = 0.71073)
2Θ range for data collection/°	2.782 to 57.61
Index ranges	$-11 \le h \le 12$, $-32 \le k \le 32$, $-25 \le l \le 24$
Reflections collected	103938
Independent reflections	10919 [Rint = 0.0678, Rsigma = 0.0368]
Data/restraints/parameters	10919/0/412
Goodness-of-fit on F^2	1.02
Final R indexes [I>=2σ (I)]	R_1 = 0.0308, wR_2 = 0.0616
Final R indexes [all data]	R_1 = 0.0492, wR_2 = 0.0676
Largest diff. peak/hole / e Å^{-3}	1.04/-0.47

D. Characterization of complex properties

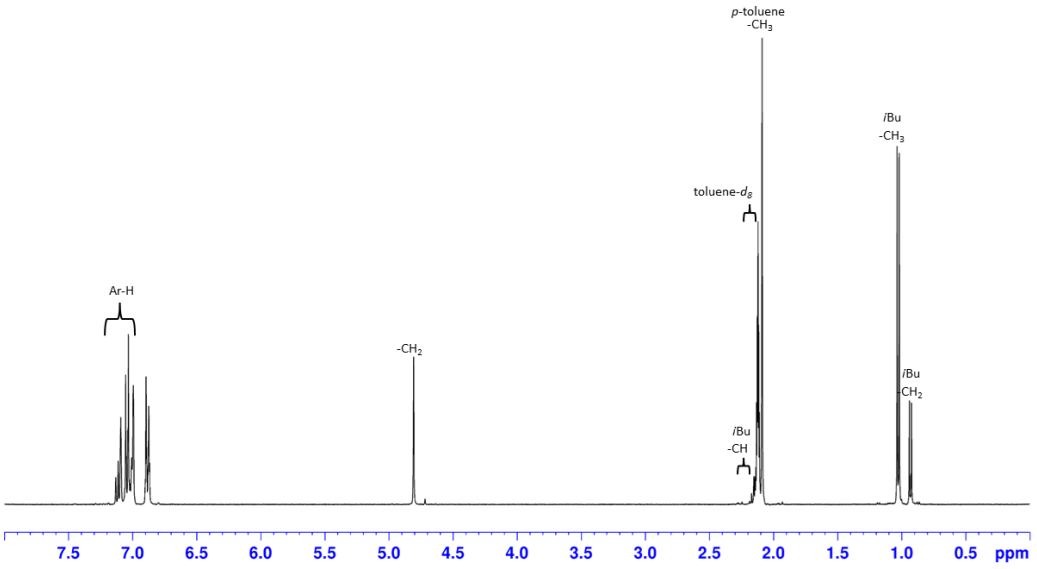

Figure S22 ^{1}H NMR spectrum of complex **1** (400 MHz, toluene-d_8, 100 °C).

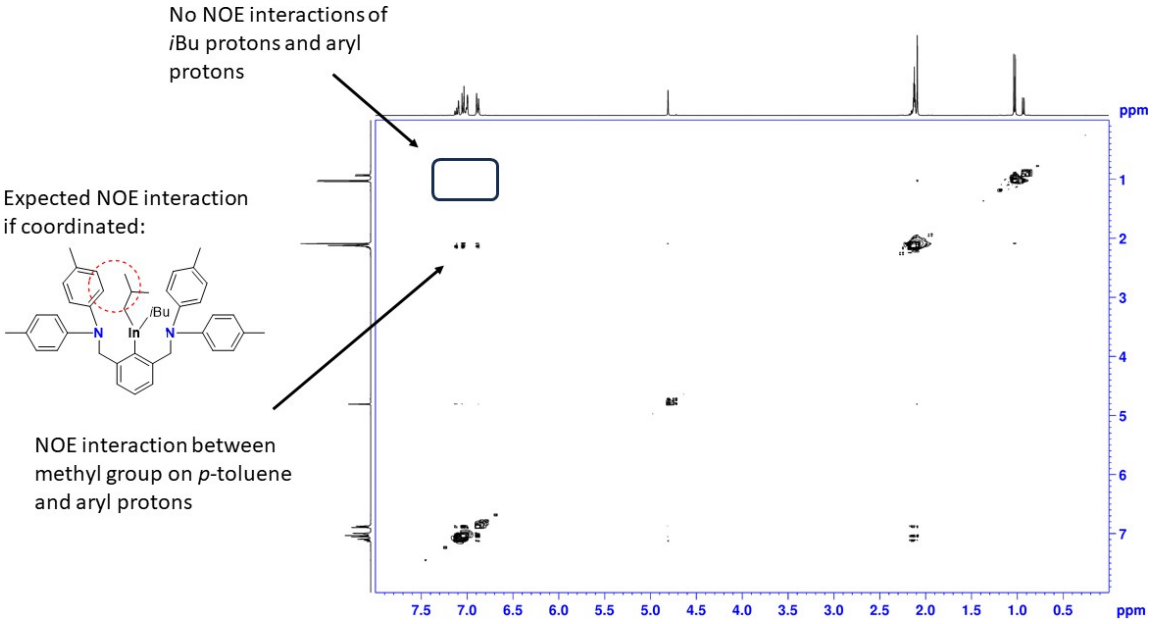

Figure S23 Nuclear Overhauser Effect spectroscopy (NOESY) NMR spectrum (400 MHz, toluene-d_8, 100 °C) of **1**

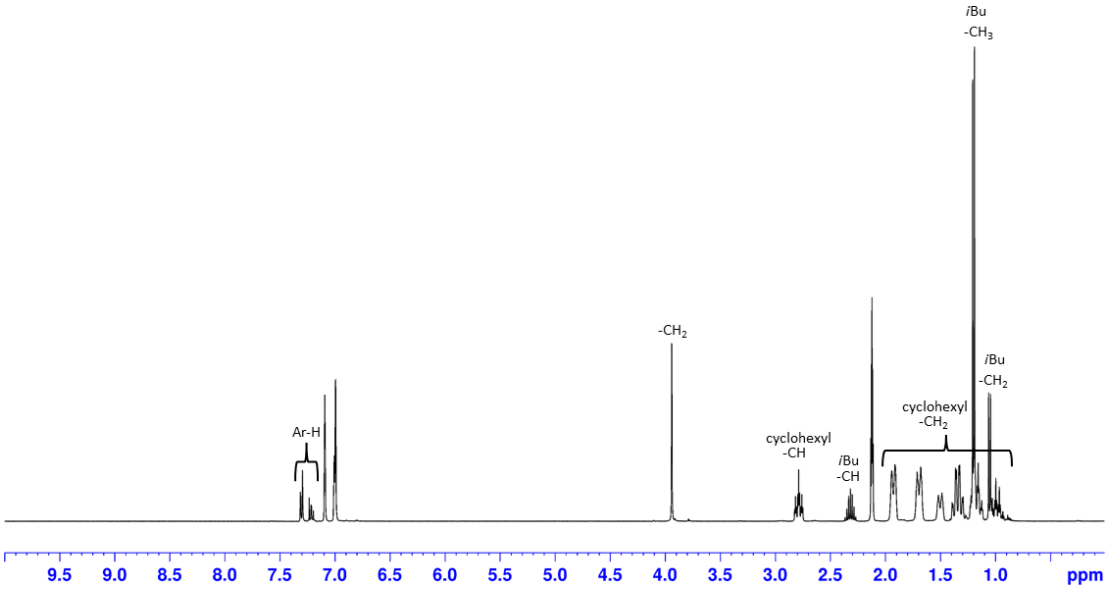

Figure S24 ^{1}H NMR spectrum of complex **2** (400 MHz, toluene-d_8, 100 °C).

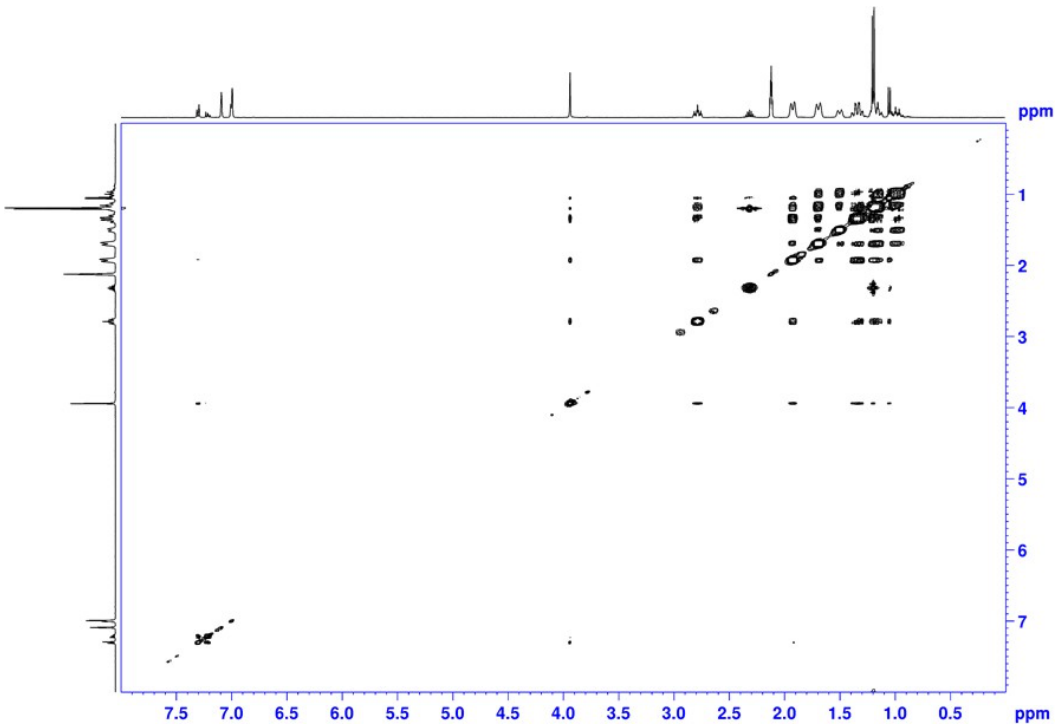

Figure S25 NOESY NMR spectrum (400 MHz, toluene-d_8, 100 °C) of **2**

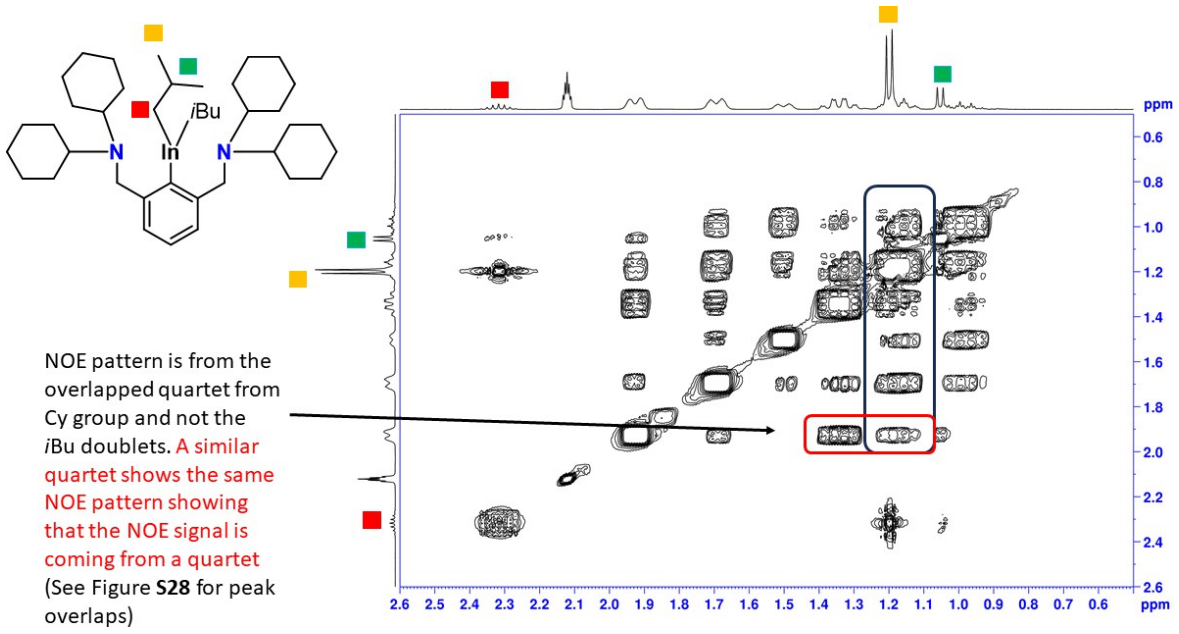

Figure S26 NOESY NMR spectrum zoomed in (400 MHz, toluene-d_8, 100 °C) of **2**

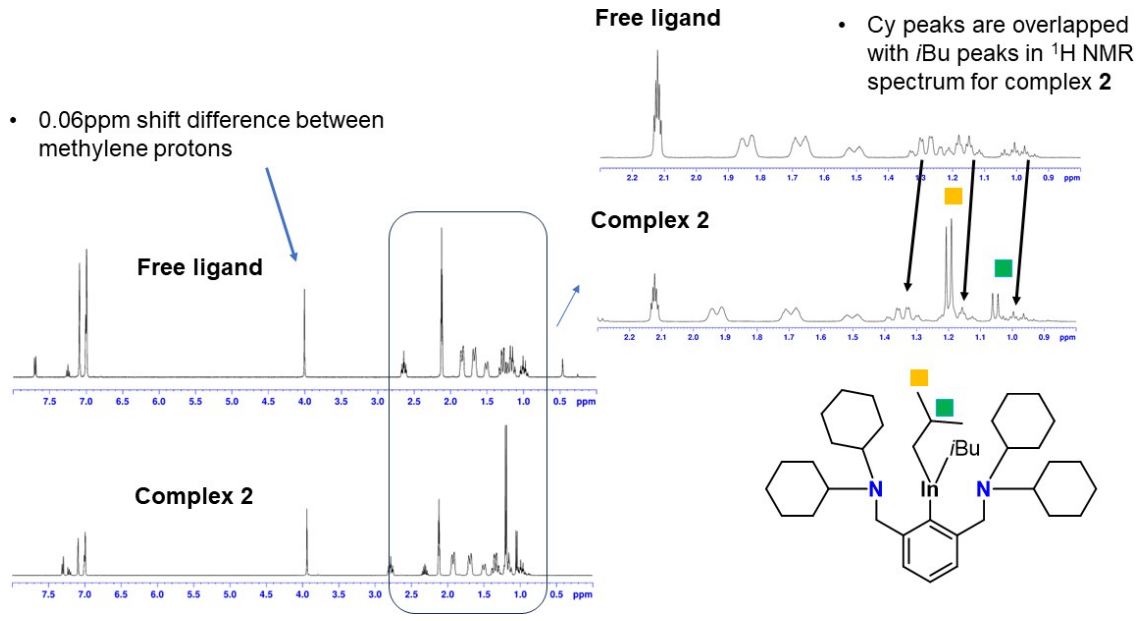

Figure S27 Comparison of ^{1}H NMR spectra of **L2** and complex **2** (400 MHz, toluene-d_8, 100 °C).

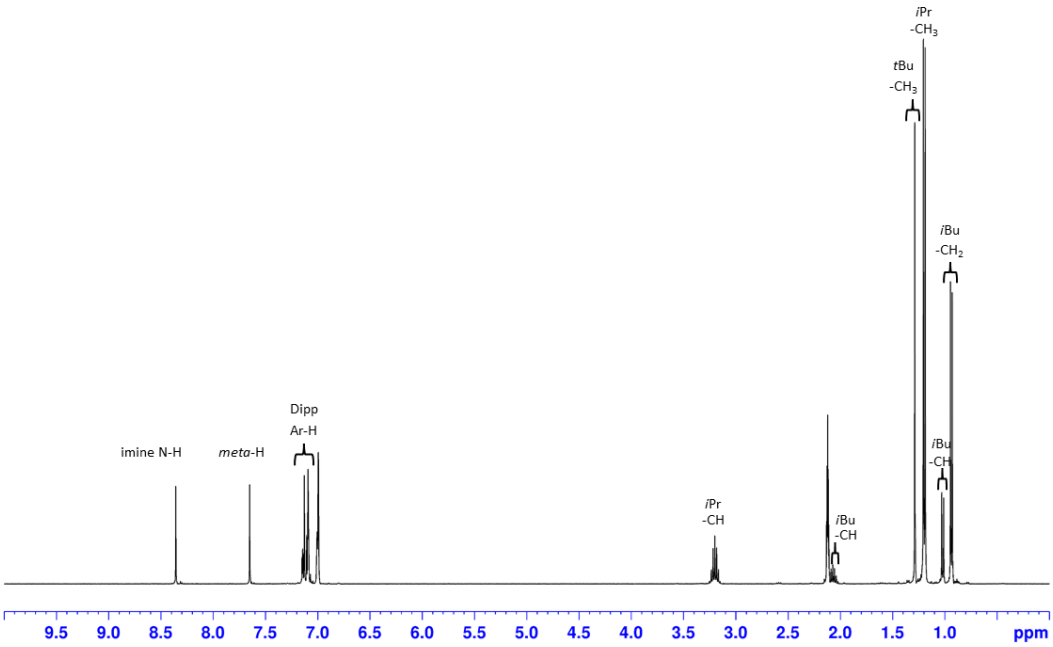

Figure S28 ^{1}H NMR spectrum of complex **3** (400 MHz, toluene-d_8, 100 °C).

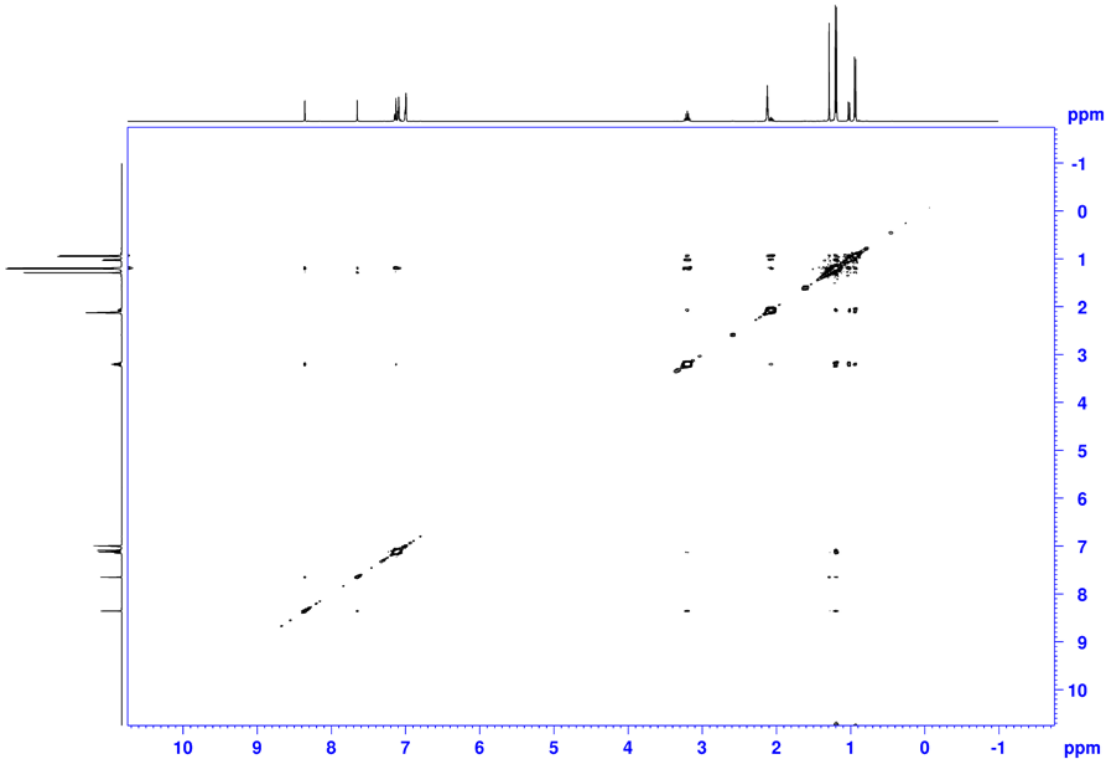

Figure S29 NOESY NMR spectrum (400 MHz, toluene-d_8, 100 °C) of **3**

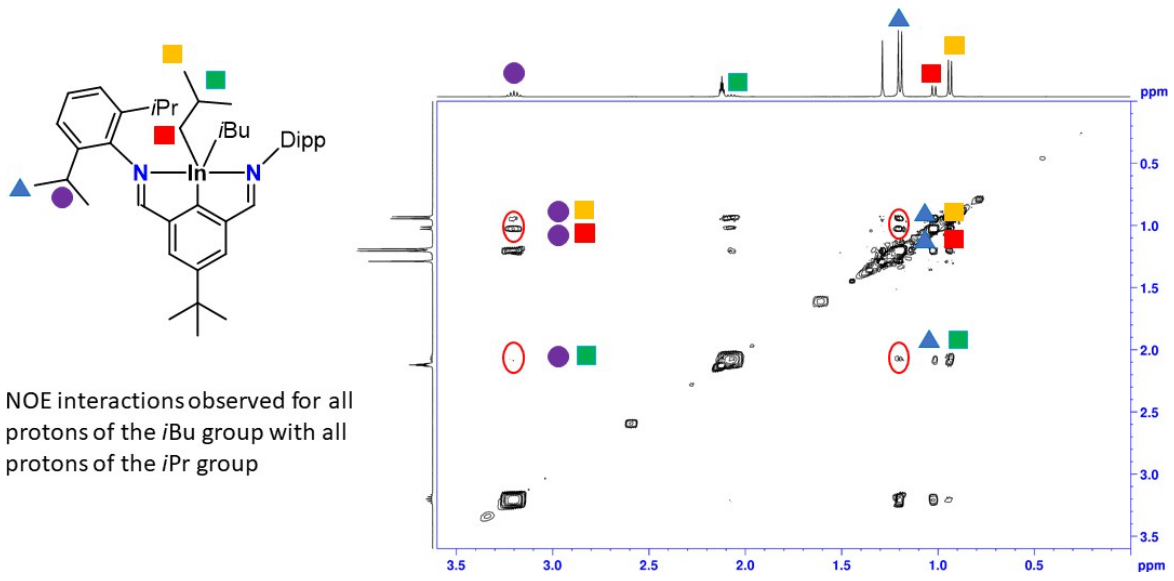

Figure S30 NOESY NMR spectrum (400 MHz, toluene-d_8, 100 °C) of **3** zoomed in

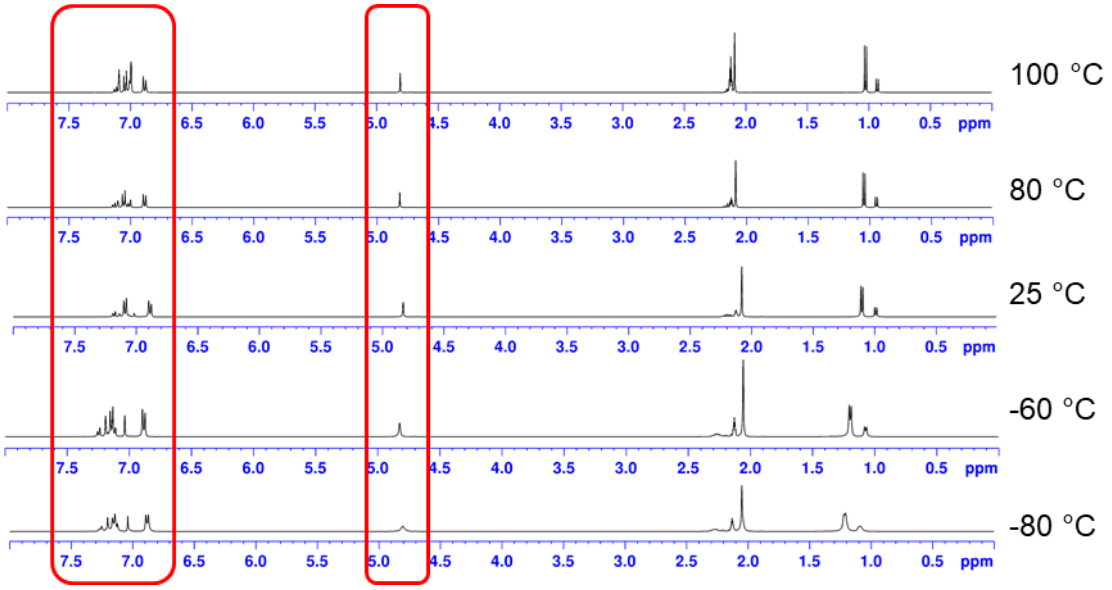

Figure S31 VT ^{1}H NMR spectra (400 MHz, toluene-d_8, −80 - 100 °C) of **1**

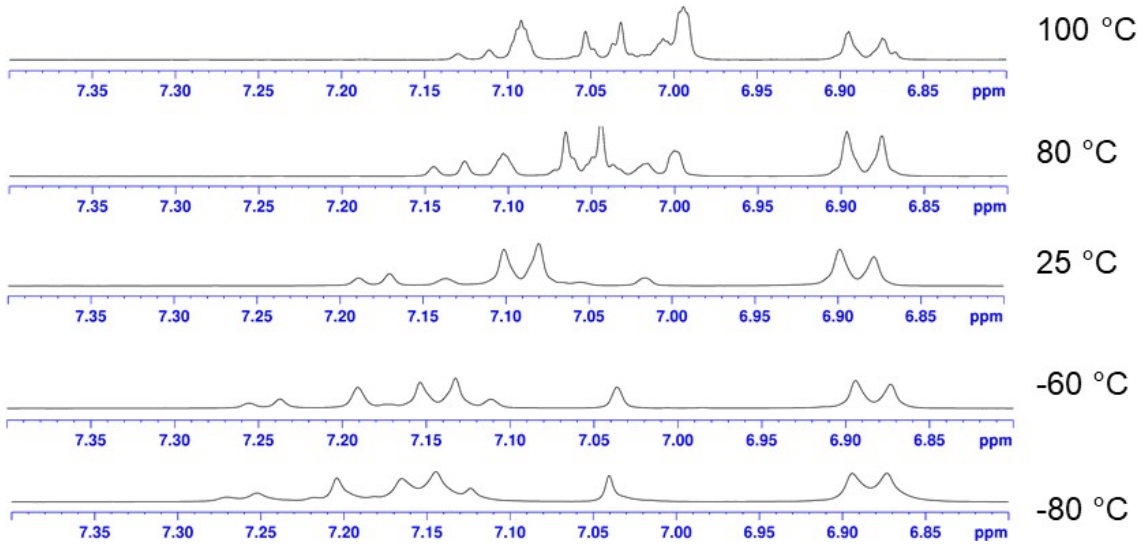

Figure S32 VT ^{1}H NMR spectra (400 MHz, toluene-d_8, −80 - 100 °C) of **1** zoomed in aryl region

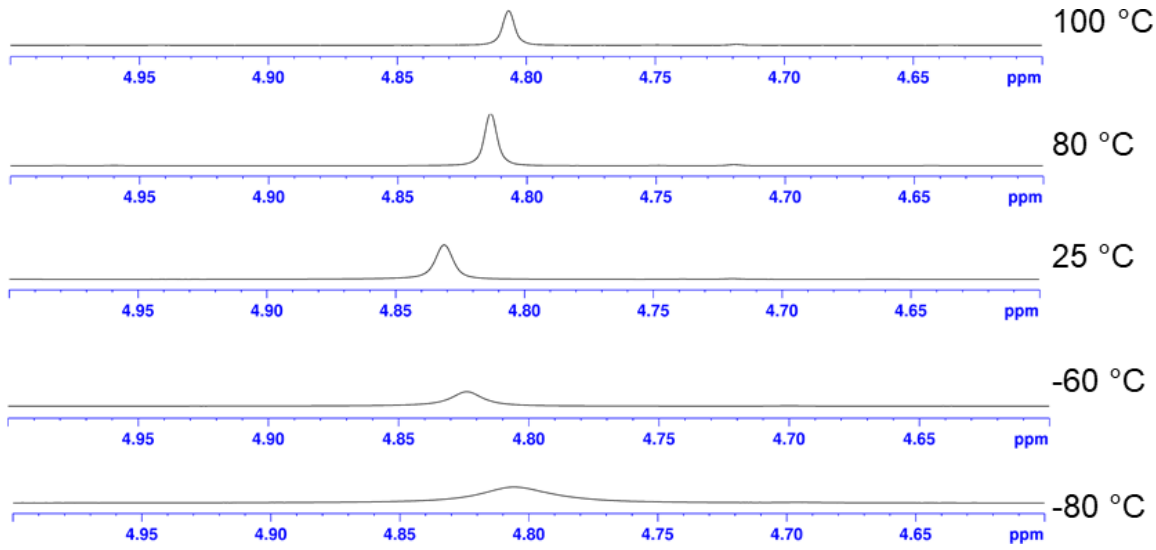

Figure S33 VT ^{1}H NMR spectra (400 MHz, toluene-d_8, −80 - 100 °C) of **1** zoomed in methylene region

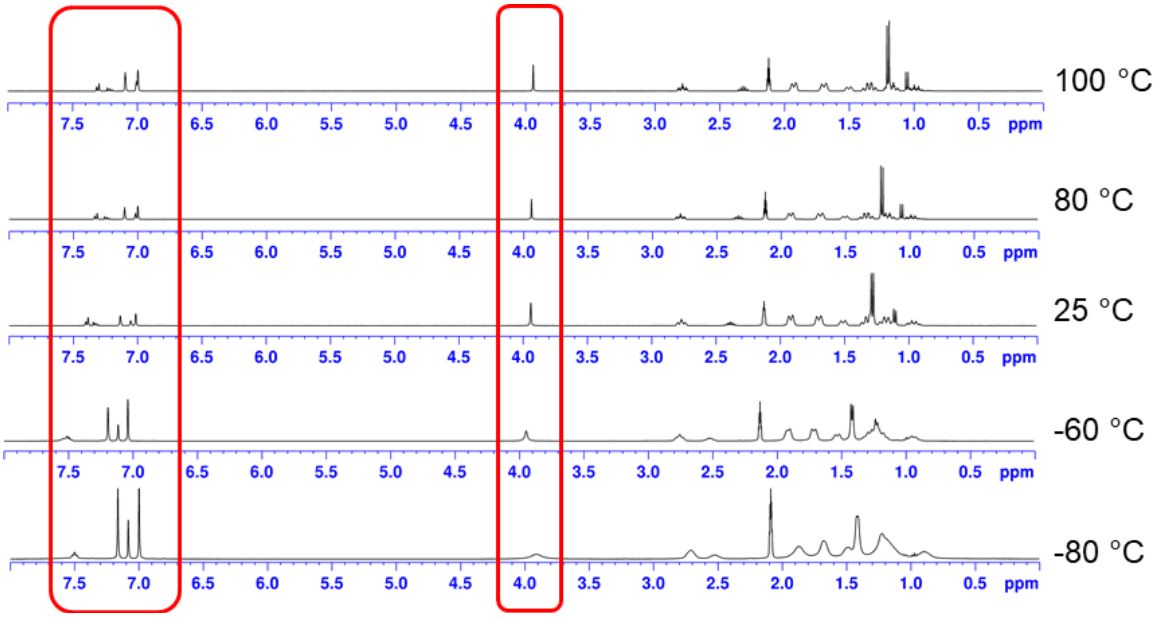

Figure S34 VT ^{1}H NMR spectra (400 MHz, toluene-d_8, −80 - 100 °C) of **2**

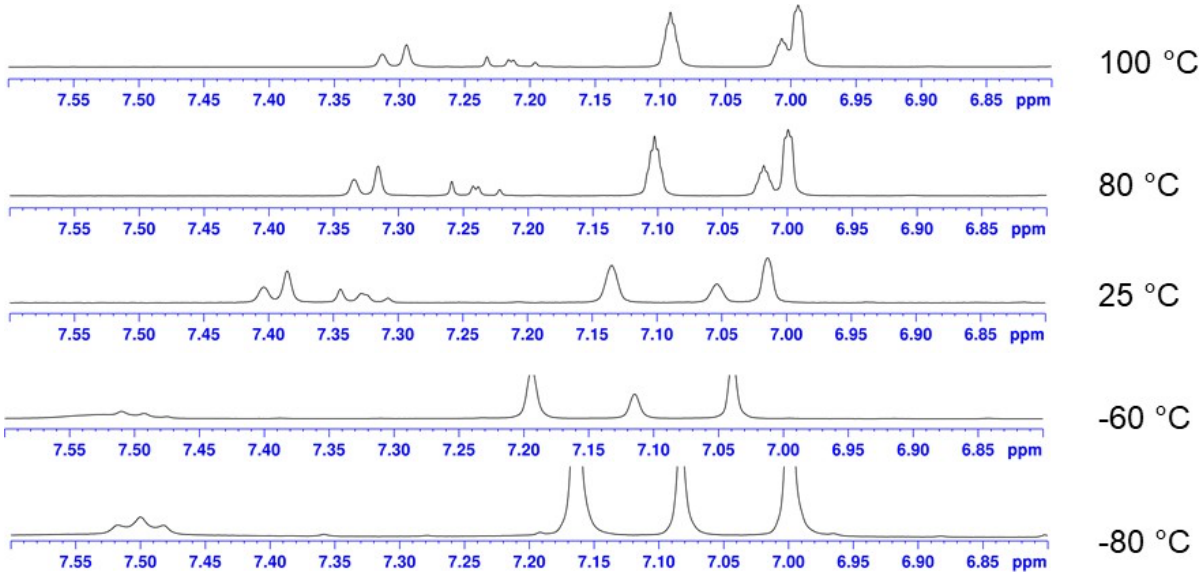

Figure S35 VT ^{1}H NMR spectra (400 MHz, toluene-d_8, −80 - 100 °C) of **2** zoomed in aryl region

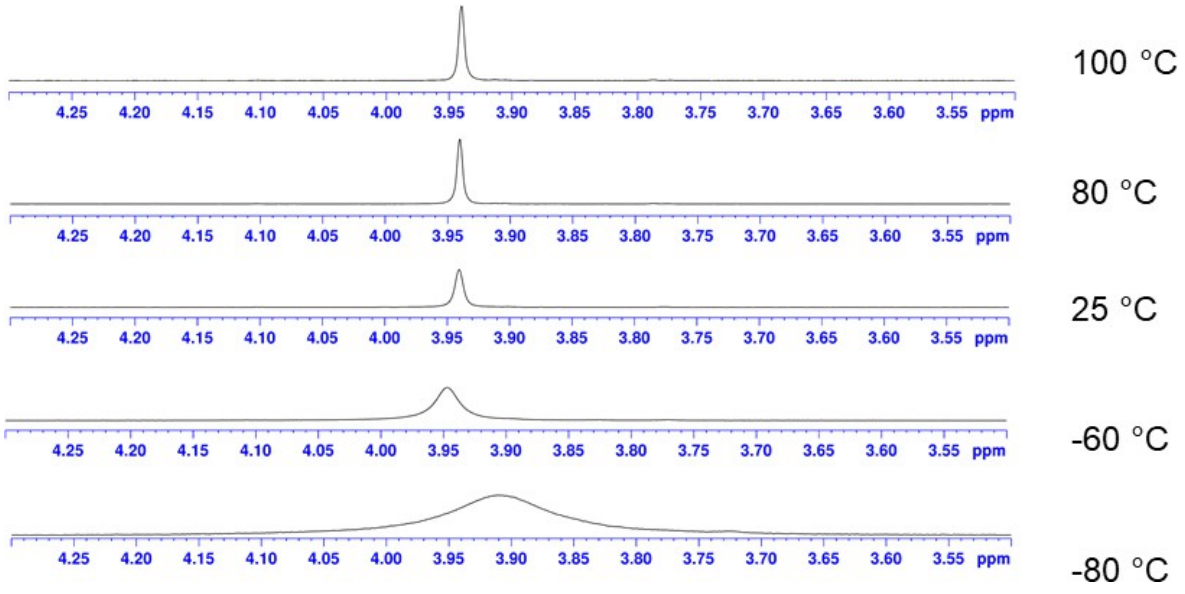

Figure S36 VT ^{1}H NMR spectra (400 MHz, toluene-d_8, −80 - 100 °C) of **2** zoomed in methylene region

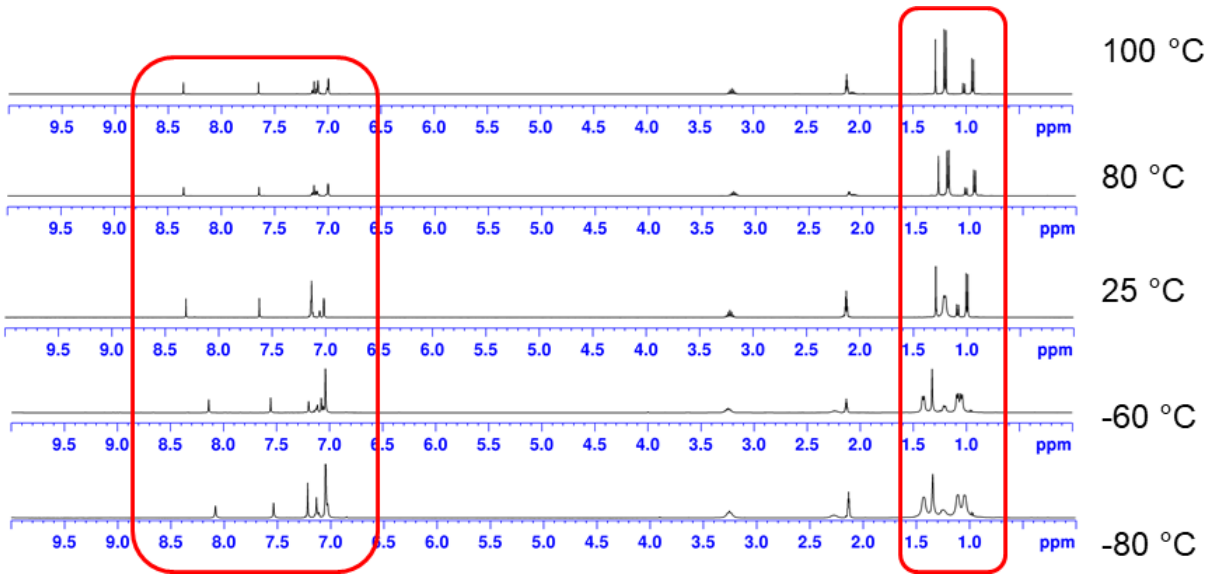

Figure S37 VT ^{1}H NMR spectra (400 MHz, toluene-d_8, −80 - 100 °C) of **3**

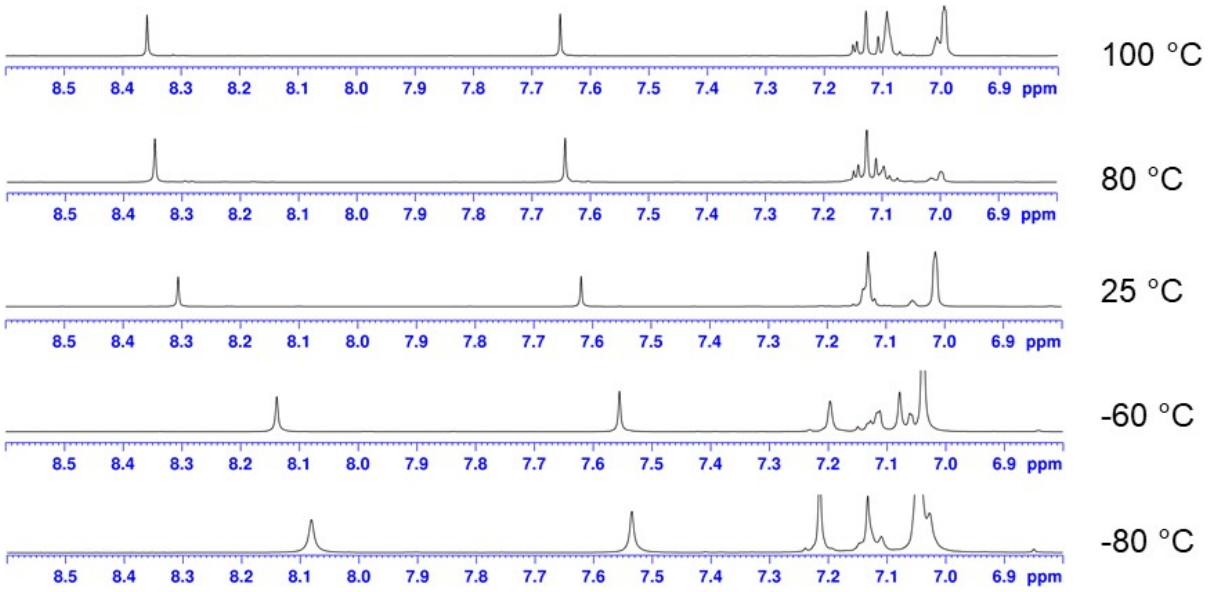

Figure S38 VT ^{1}H NMR spectra (400 MHz, toluene-d_8, −80 - 100 °C) of **3** zoomed in aryl/imine region

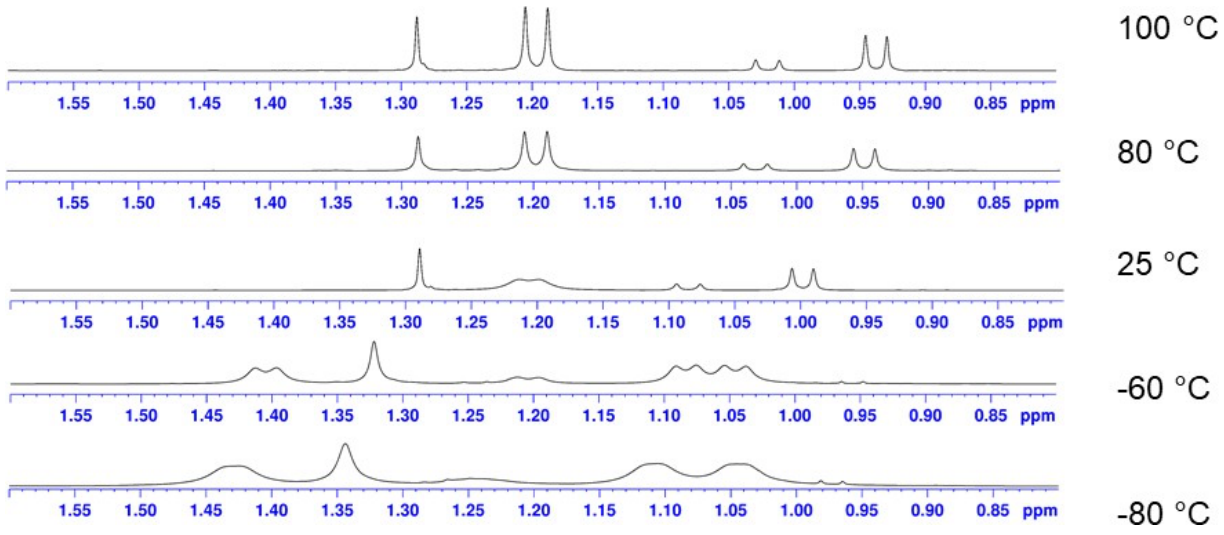

Figure S39 VT ^{1}H NMR spectra (400 MHz, toluene-d_8, −80 - 100 °C) of **3** zoomed in *i*Pr region

E. Polymerization and polymer characterization

Table S6 Polymerization of *rac*-LA using initiators **1-3** with varying monomer ratios

Entry	Init	[M]:[I]	Temp (°C)	Time (min)	Conv (%)	$M_{n,\,theo}$ (kg/mol)	$M_{n,\,SEC}$ (kg/mol)	$Đ$
1	**1**	100	100	30	**82**	**11.8**	**40.5**	**1.47**
2	**1**	200	100	30	**88**	**25.4**	**83.0**	**1.56**
3	**1**	300	100	30	**85**	**36.8**	**61.3**	**1.54**
4	**1**	400	100	30	**87**	**50.2**	**54.4**	**1.58**
5	**2**	100	100	30	**81**	**11.7**	**53.6**	**1.72**
6	**2**	200	100	30	**82**	**23.6**	**129.7**	**1.66**
7	**2**	300	100	30	**72**	**31.1**	**97.9**	**1.68**
8	**2**	400	100	30	**60**	**34.6**	**104.1**	**1.71**
9	**3**	100	100	30	**32**	**4.62**	**38.3**	**1.30**
10	**3**	200	100	30	**34**	**9.8**	**54.9**	**1.60**
11	**3**	300	100	30	**32**	**13.8**	**87.5**	**1.39**
12	**3**	400	100	30	**27**	**15.6**	**111.7**	**1.28**

[a]All reactions were carried out in 0.5 mL toluene [Initiator 1-3] = 0.014 M. [b]Conversions were determined by analyzing the ^{1}H NMR spectra (300 MHz, $CDCl_3$, 25 °C) of the crude mixtures. [c]$M_{n,\,theo}$ values were calculated by [M]:[I] × conversion × 144.13. [d]$M_{n,\,SEC}$ determined using SEC in THF.

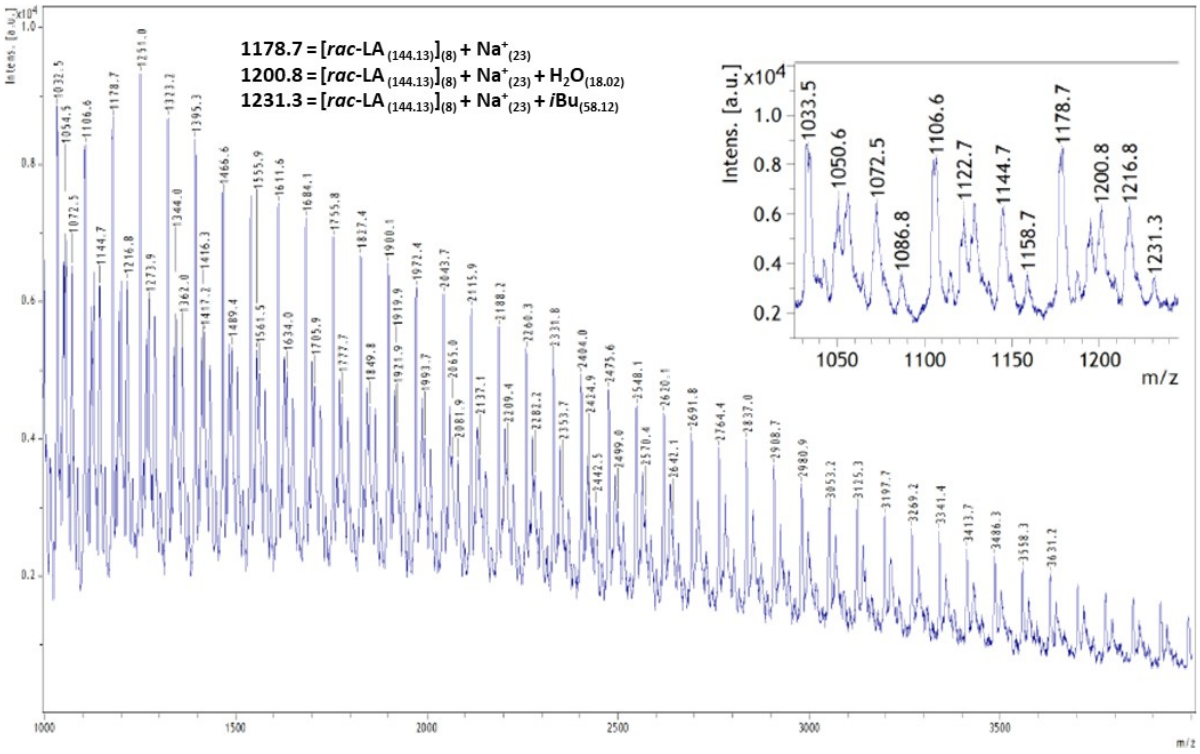

Figure S40 MALDI-TOF spectrum of PLA from polymerization of *rac*-LA with complex **1**

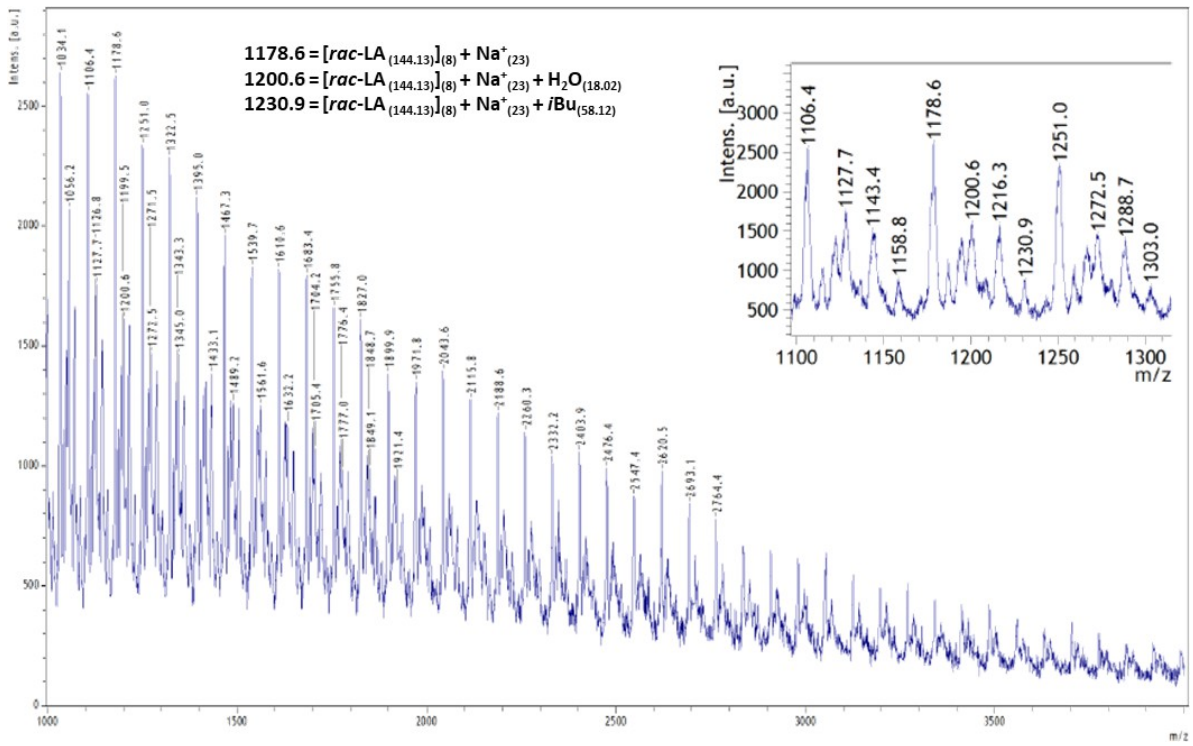

Figure S41 MALDI-TOF spectrum of PLA from polymerization of *rac*-LA with complex **2**

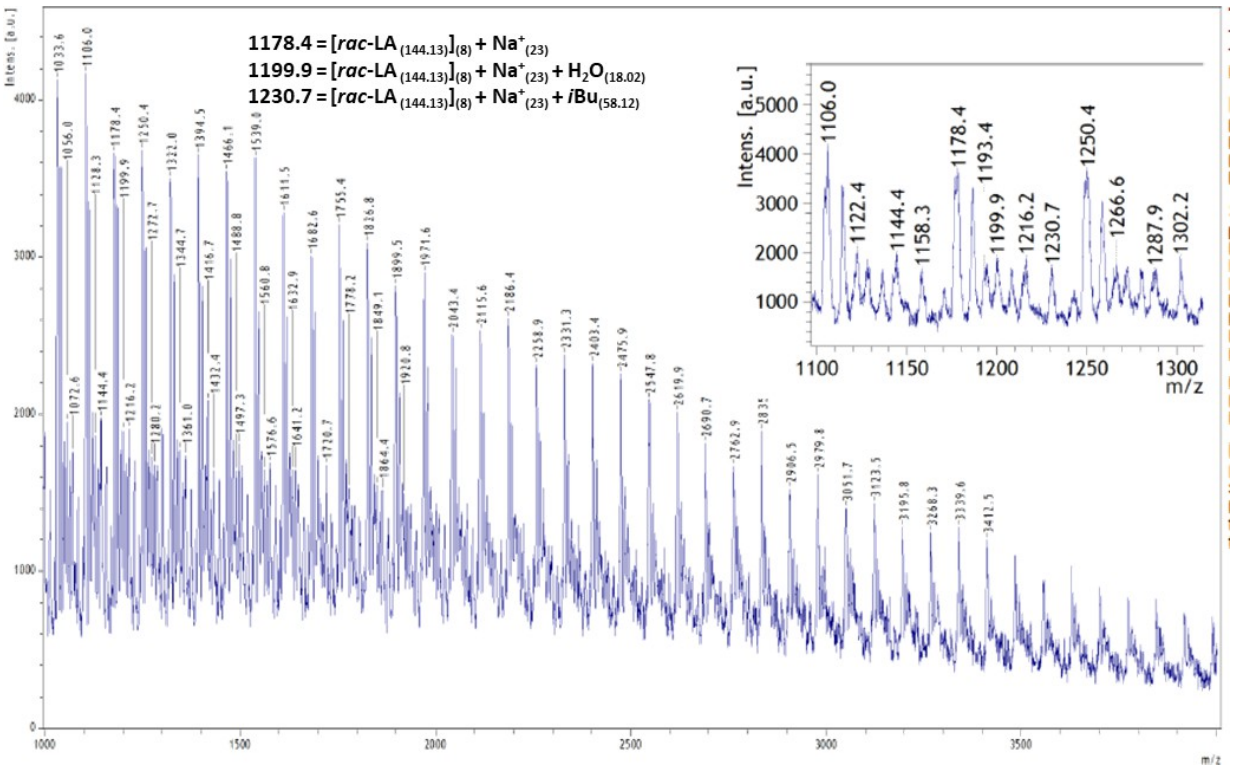

Figure S42 MALDI-TOF spectrum of PLA from polymerization of *rac*-LA with complex **3**

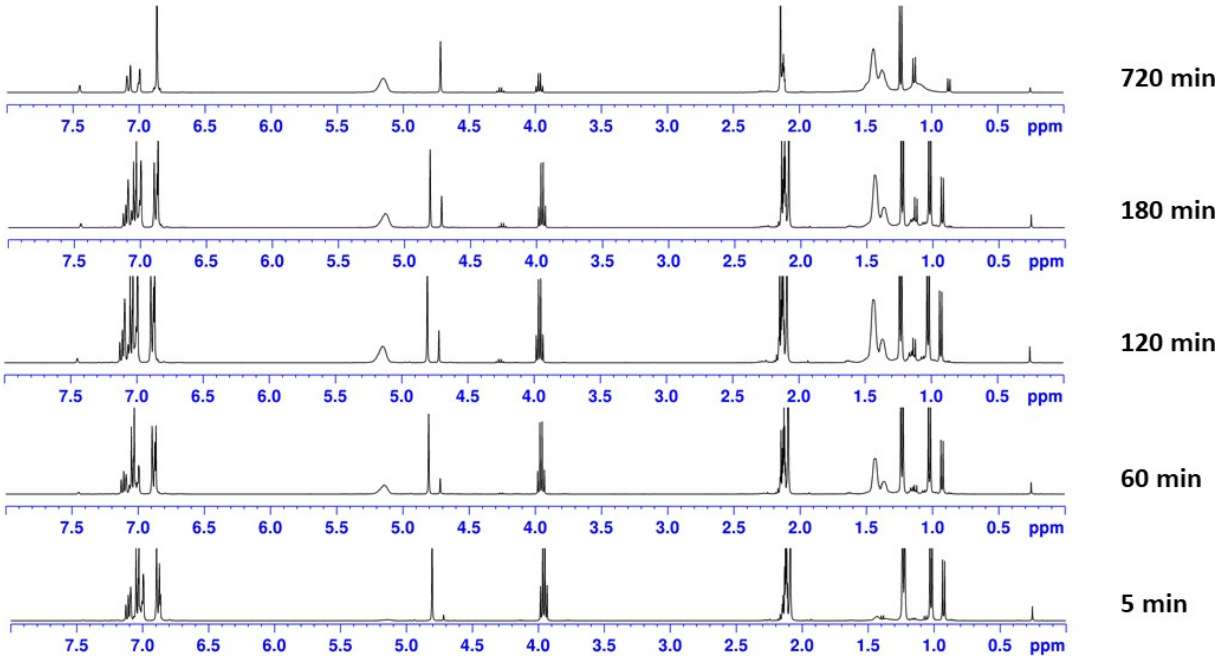

Figure S43 *In situ* monitoring of ^{1}H NMR spectra of the oligomerization of 5 equiv *rac*-LA using **1** (400 MHz, toluene-d_8, 100 °C).

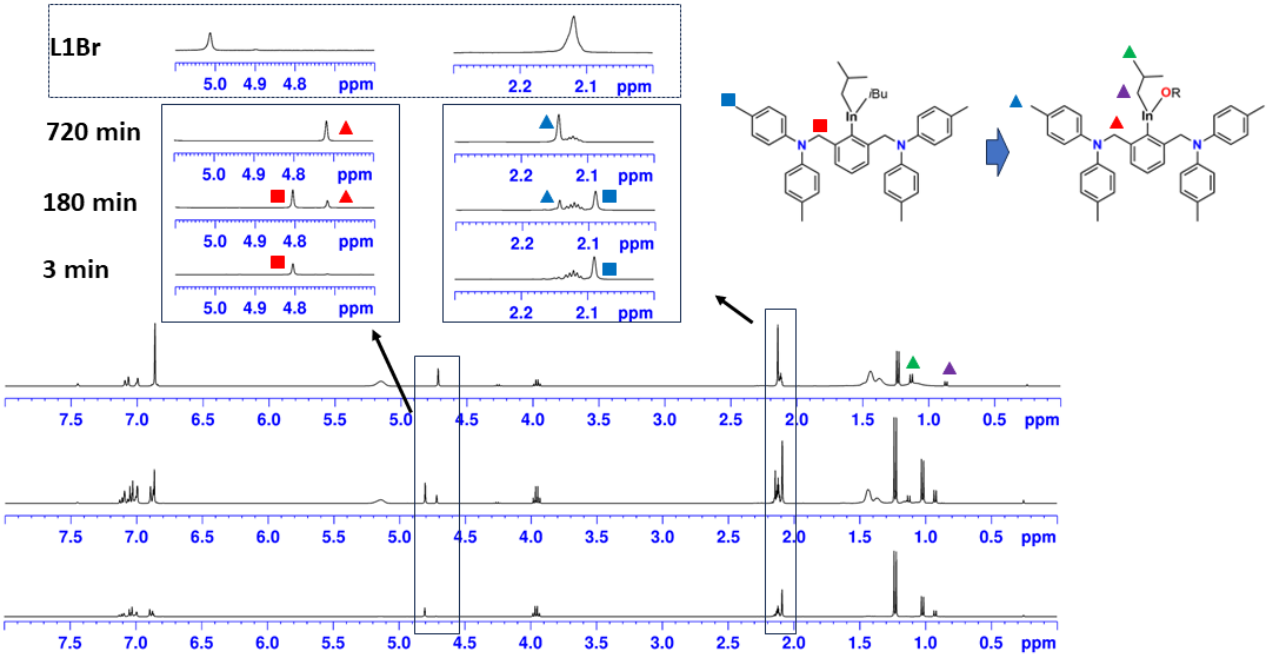

Figure S44 *In situ* monitoring of ^{1}H NMR spectra of the oligomerization of 5 equiv *rac*-LA using **1** zoomed in to show the propagating alkoxide complex (400 MHz, toluene-d_8, 100 °C).

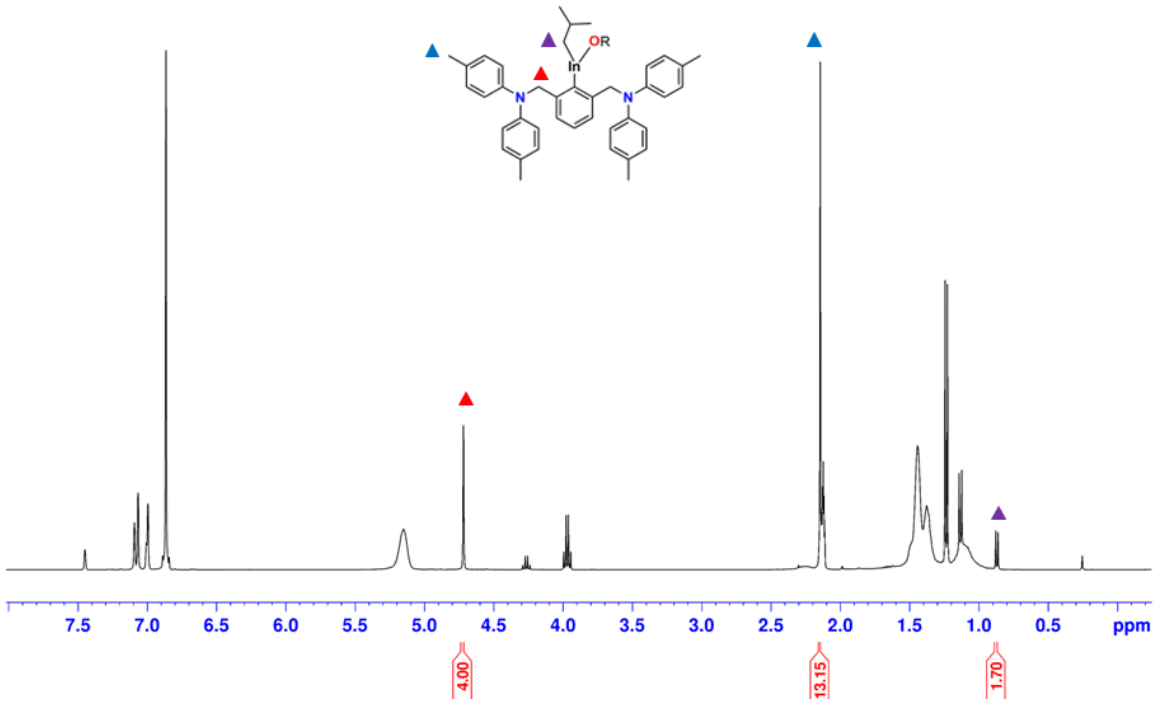

Figure S45 ^{1}H NMR spectrum of the oligomerization of 5 equiv *rac*-LA using **1** after 720 minutes (400 MHz, toluene-d_8, 100 °C).

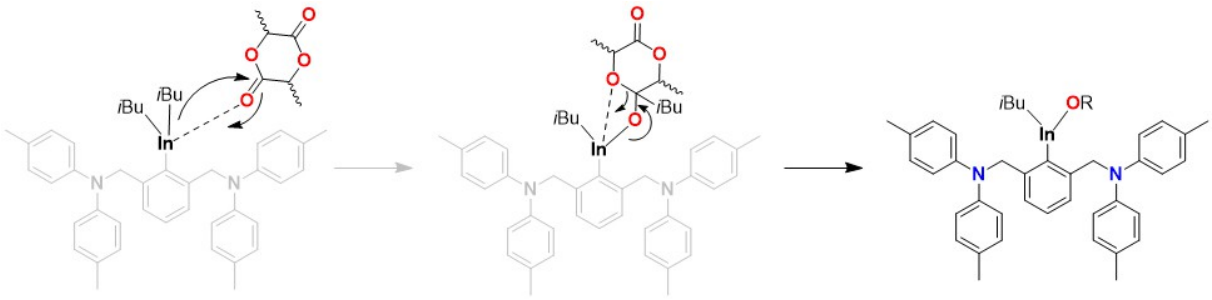

Figure S46 Proposed mechanism for the formation of the alkoxide species generated *in situ*

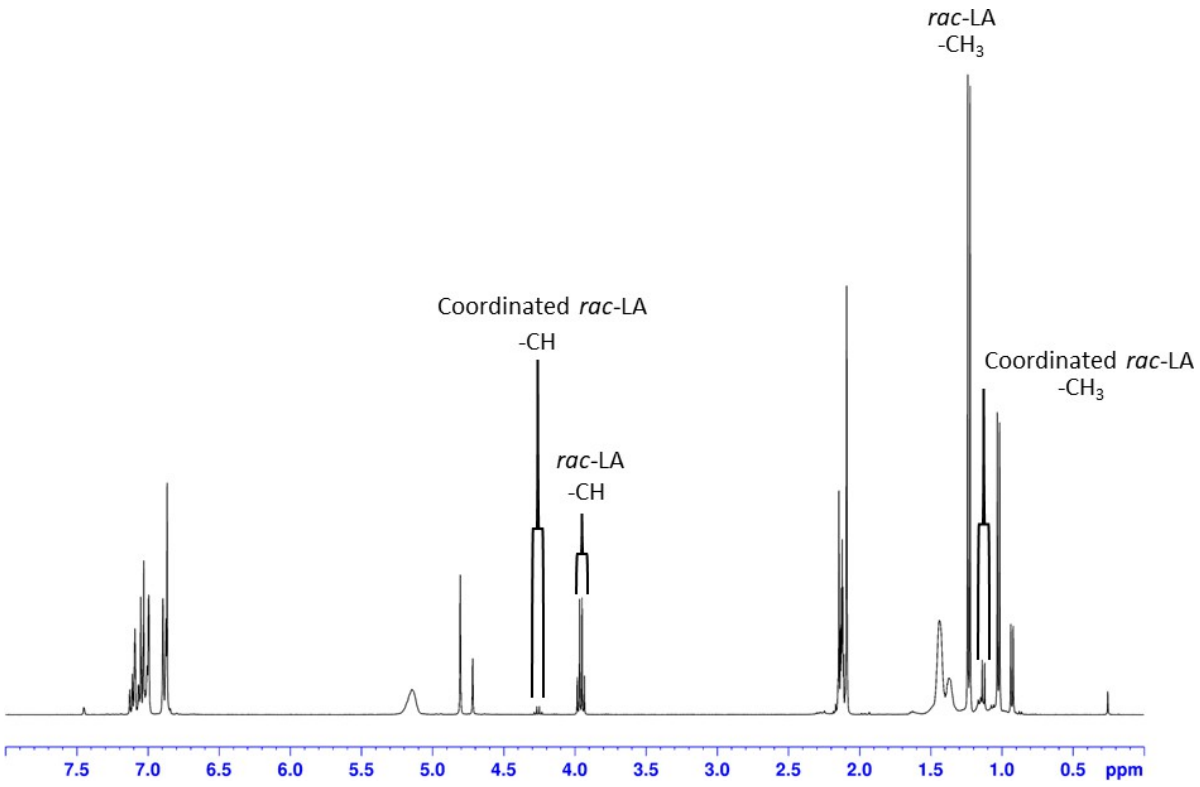

Figure S47 ^{1}H NMR spectrum showing the coordination of *rac*-LA to **1** (400 MHz, toluene-d_8, 100 °C).

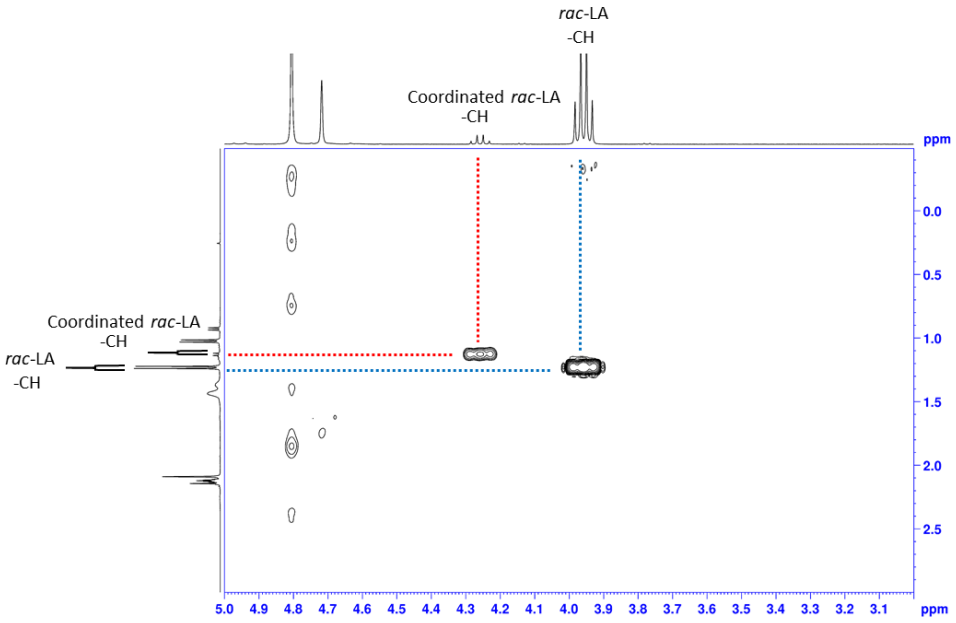

Figure S48 ^{1}H-^{1}H COSY NMR spectrum showing the coordination of *rac*-LA to **1** zoomed in (400 MHz, toluene-d_8, 100 °C).

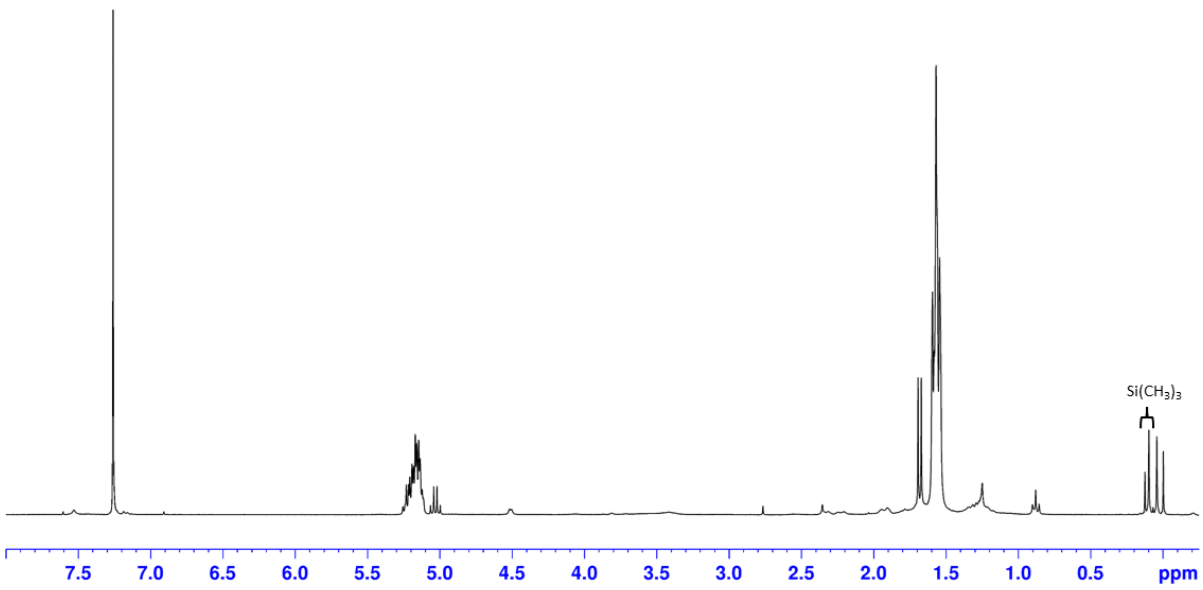

Figure S49 ^{1}H NMR spectrum of the oligomerization of 5 equiv *rac*-LA using **4** (400 MHz, $CDCl_3$, 25 °C).

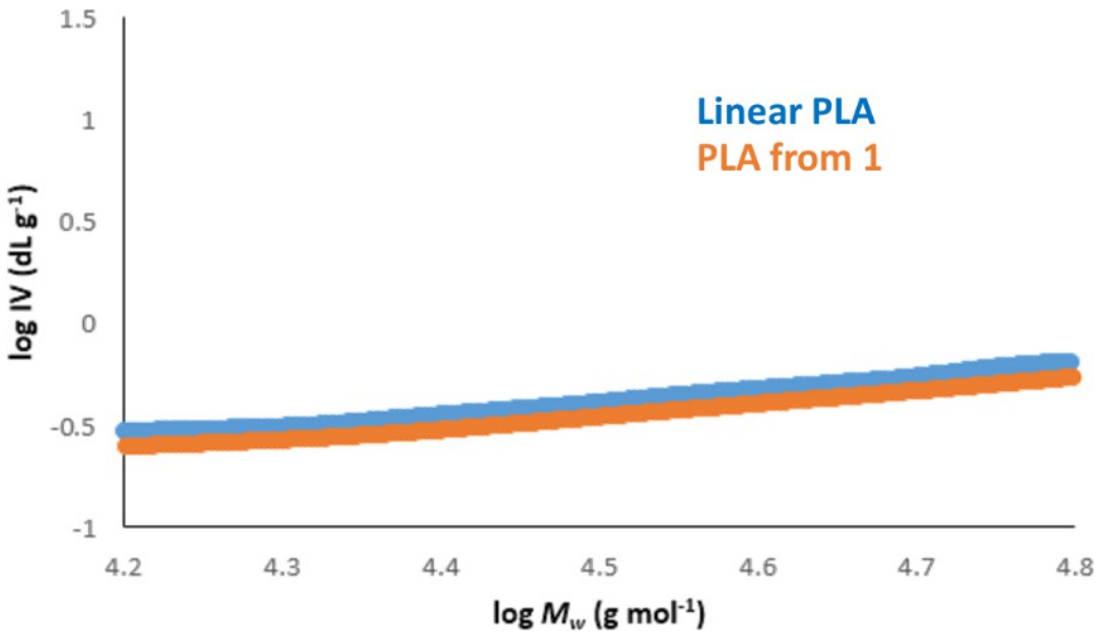

Figure S50 Mark-Houwink plots for PLA (Table 1, entry 7) and linear PLA (Table S7, entry 1)

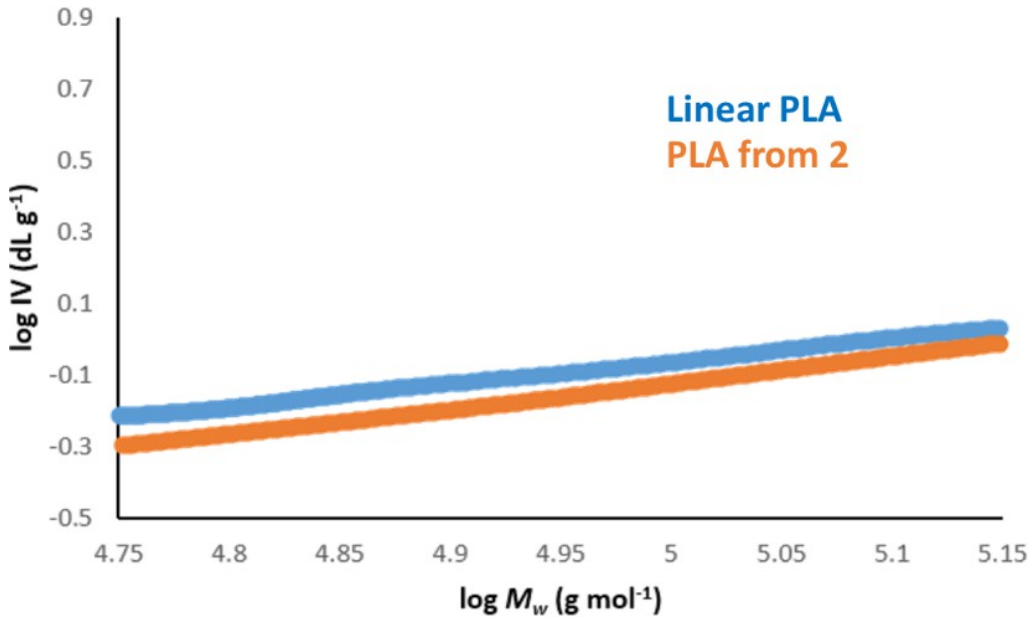

Figure S51 Mark-Houwink plots for PLA (Table 1, entry 8) and linear PLA (Table S7, entry 2)

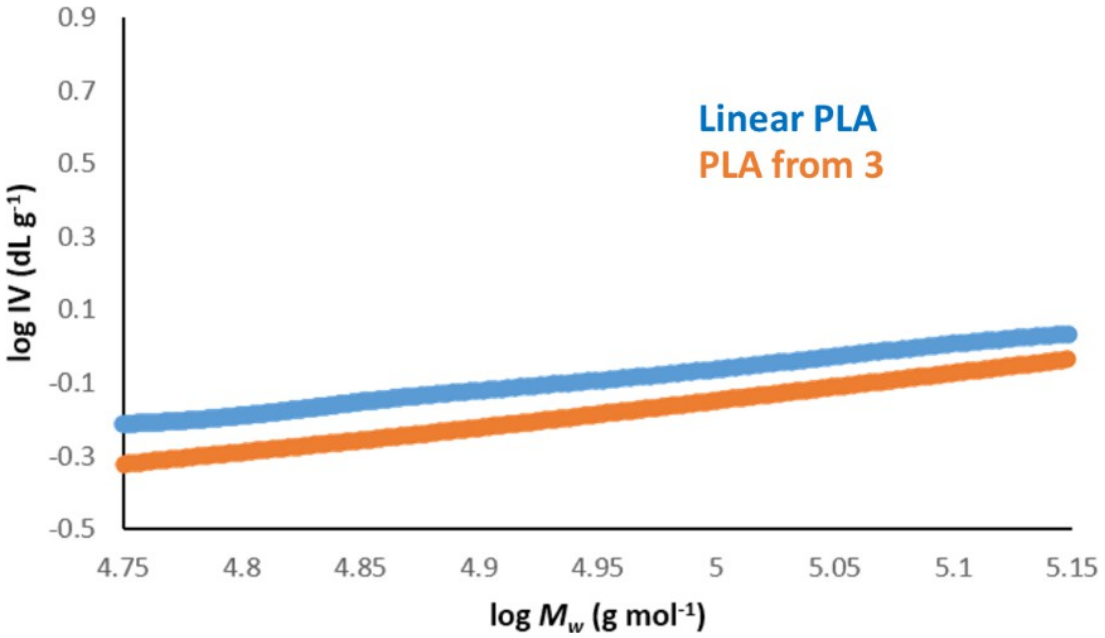

Figure S52 Mark-Houwink plots for PLA (Table 1, entry 9) and linear PLA (Table S7, entry 2)

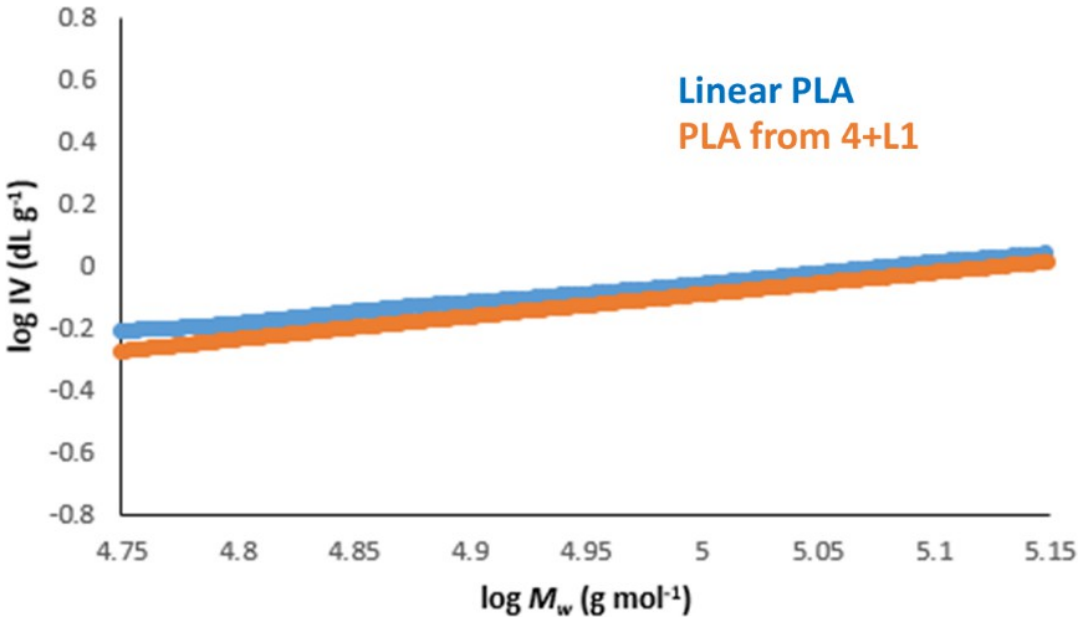

Figure S53 Mark-Houwink plots for PLA (Table 2, entry 3) and linear PLA (Table S7, entry 2)

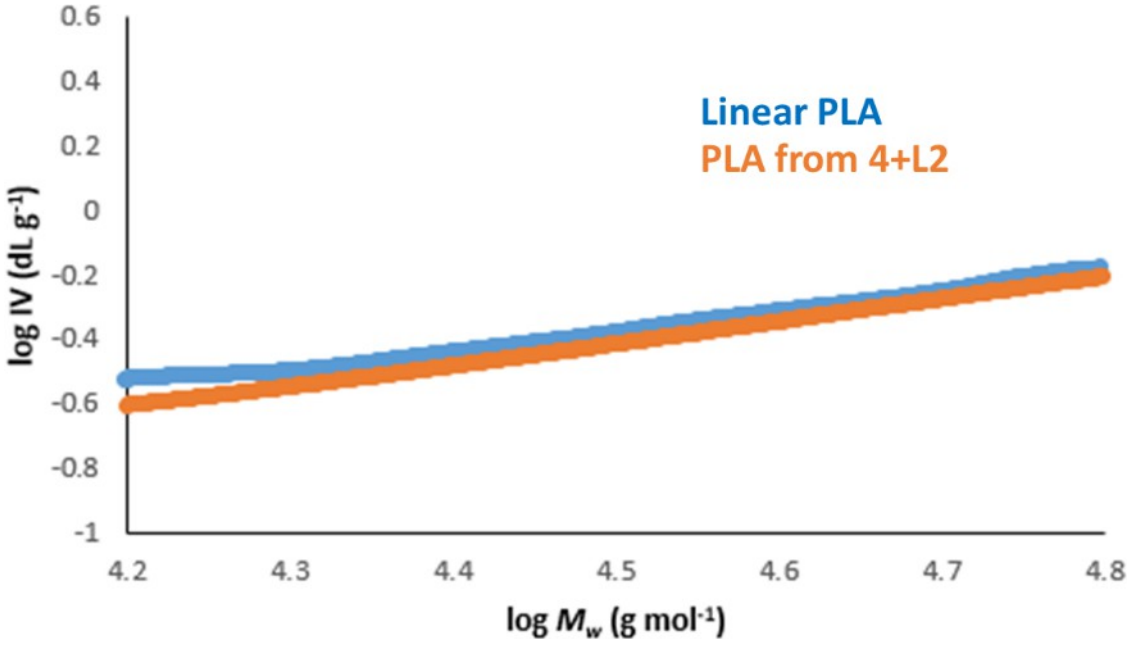

Figure S54 Mark-Houwink plots for PLA (Table 2, entry 4) and linear PLA (Table S7, entry 1)

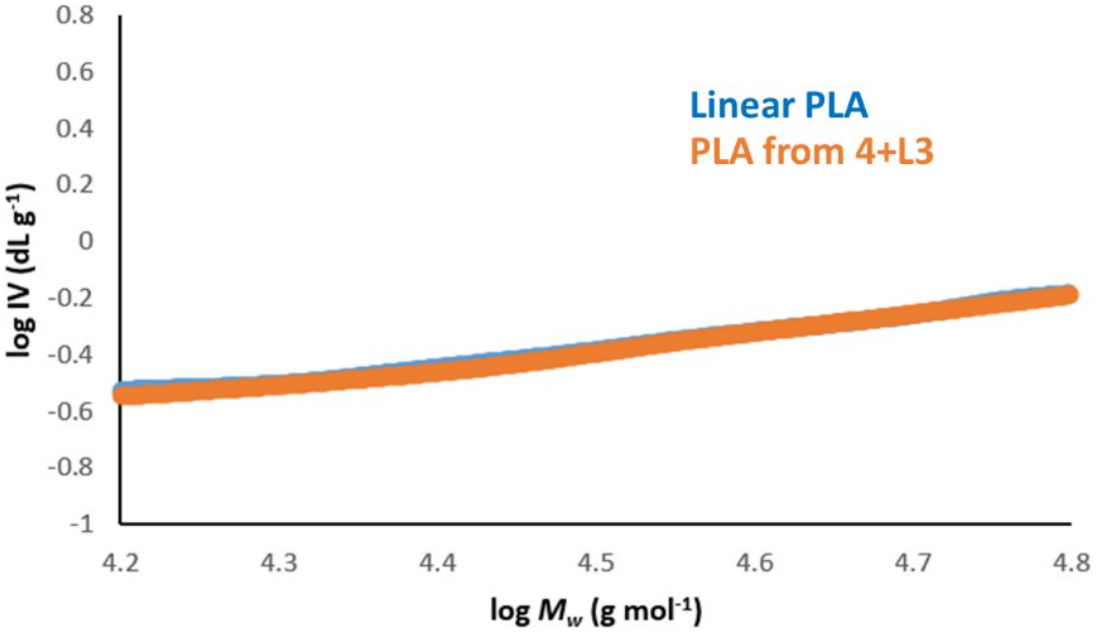

Figure S55 Mark-Houwink plots for PLA (Table 2, entry 5) and linear PLA (Table S7, entry 1)

Table S7 Synthesis of linear PLA using a previously reported dinuclear indium alkoxide catalyst.[5]

Entry	[M]:[I]	Time (h)	Conv.	M_n	$Đ$
1	200	4	>99	34.7	1.15
2	500	4	>99	74.6	1.06

[a]Reactions were performed in DCM at 25 ° C. [b]Conversions were determined by ^{1}H NMR spectroscopy. [c]M_n determined through SEC in THF. [d]Dispersity = M_w/M_n

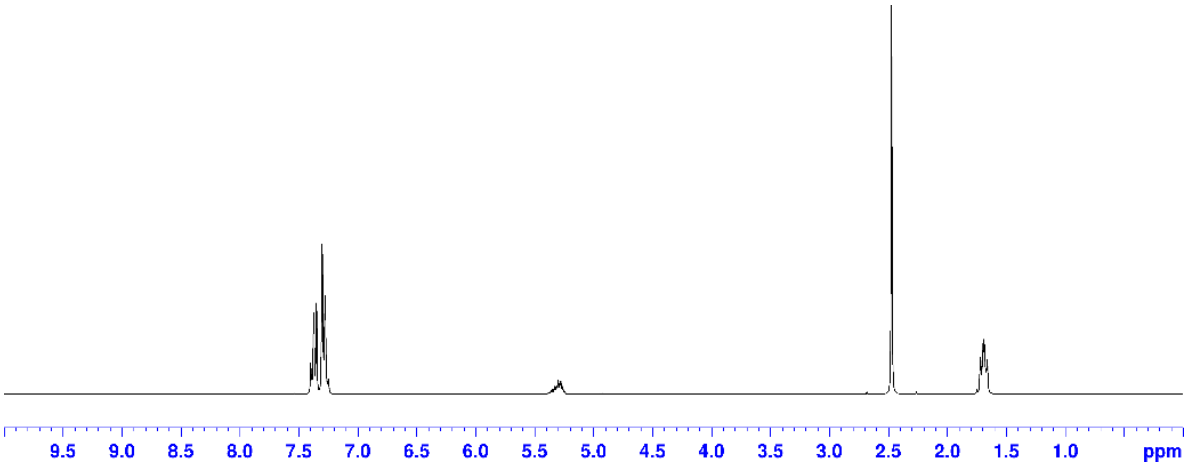

Figure S56 Representative ^{1}H NMR spectrum of PLA produced with **1** (Table 1, entry 7) (300 MHz, toluene-d_8, 25 °C).

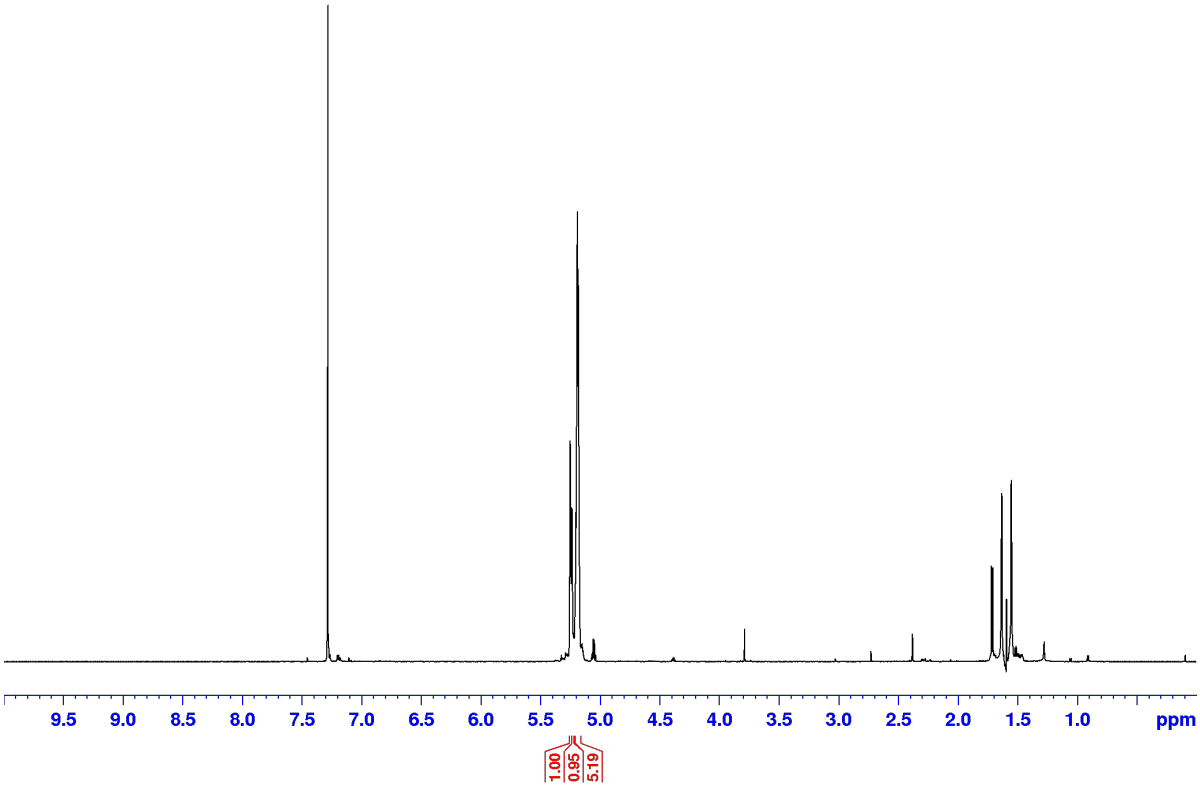

Figure S57 $^{1}H\{^{1}H\}$ NMR spectrum of PLA (after precipitation) produced with **1** (Table S6, entry 4) (600 MHz, $CDCl_3$, 25 °C). $P_r = 0.53$ and $P_m = 0.50$.

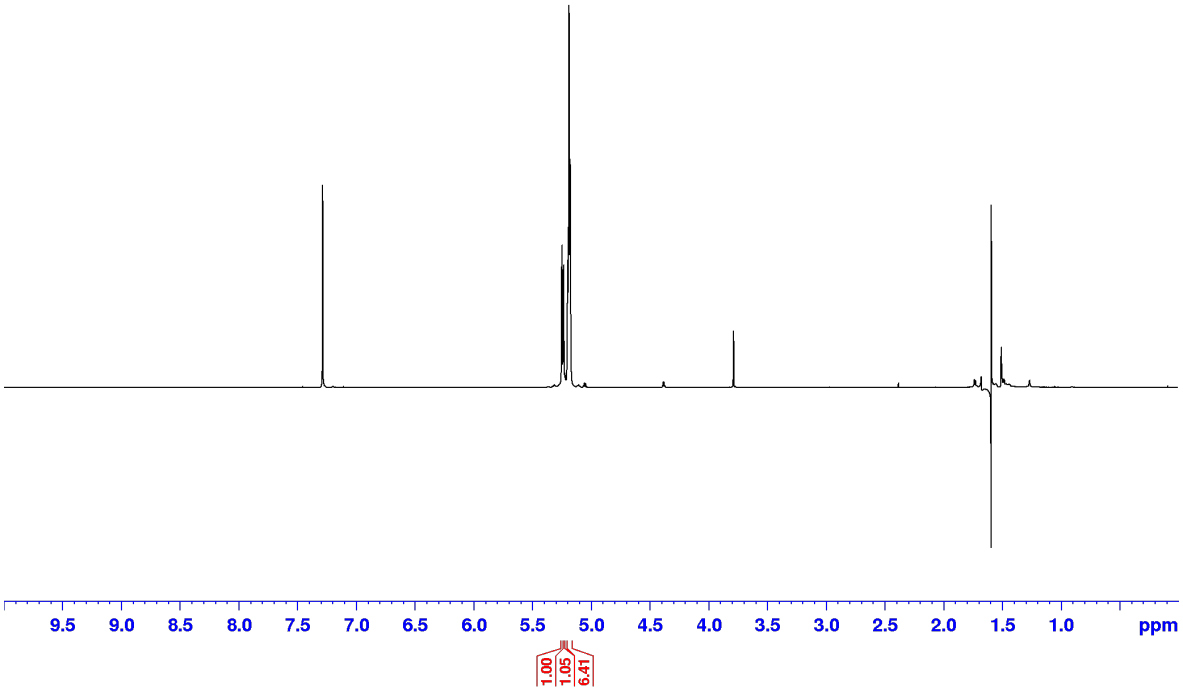

Figure S58 $^{1}H\{^{1}H\}$ NMR spectrum of PLA (after precipitation) produced with **2** (Table S6, entry 8) (600 MHz, $CDCl_3$, 25 °C). $P_r = 0.48$ and $P_m = 0.51$.

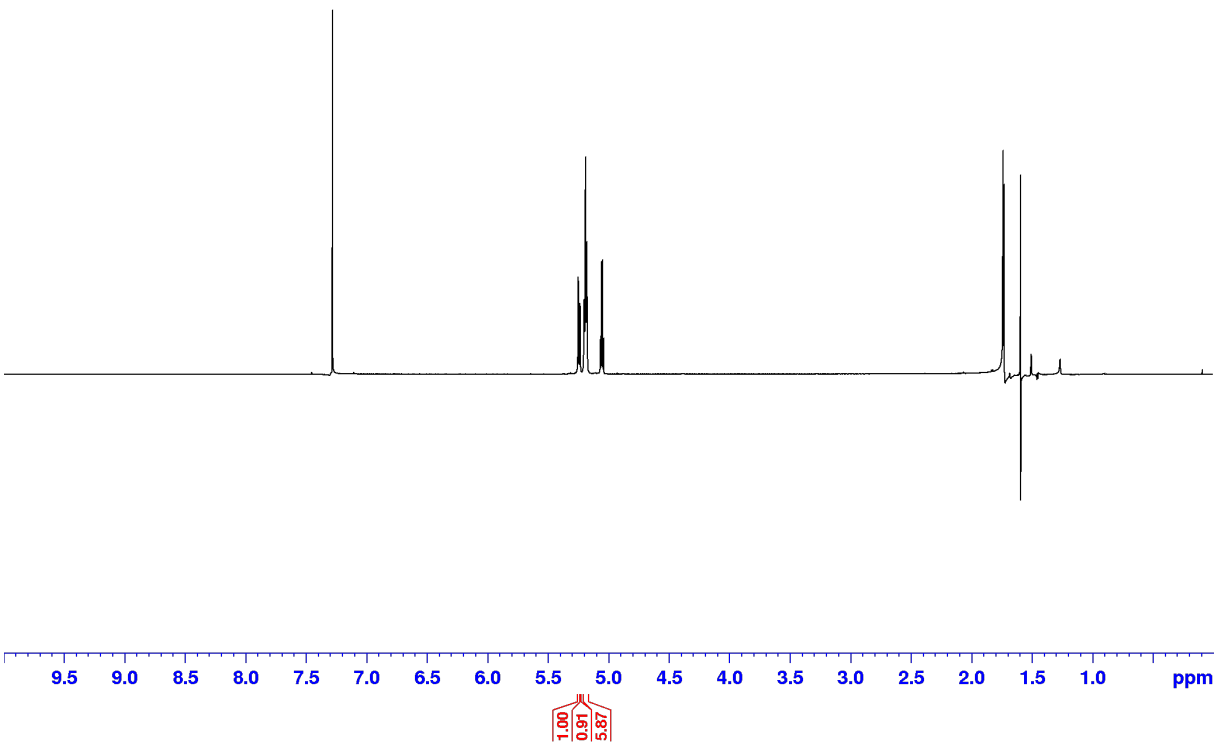

Figure S59 $^{1}H\{^{1}H\}$ NMR spectrum of PLA (after precipitation) produced with **3** (Table S6, entry 12) (600 MHz, $CDCl_3$, 25 °C). $P_r = 0.50$ and $P_m = 0.46$.

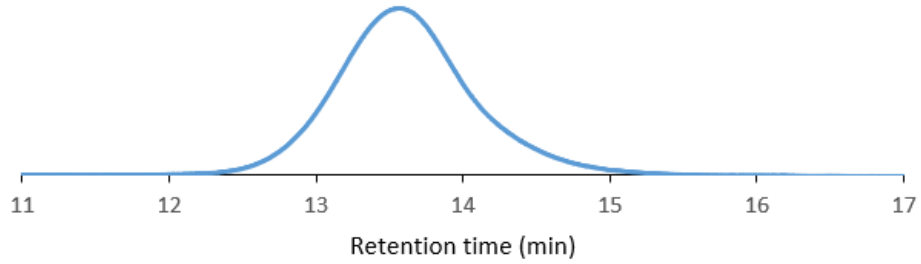

Figure S60 SEC trace of PLA (Table 1, entry 1)

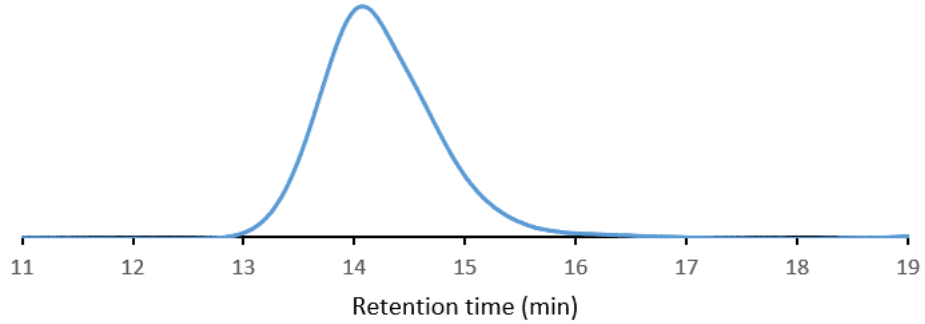

Figure S61 SEC trace of PLA (Table 1, entry 2)

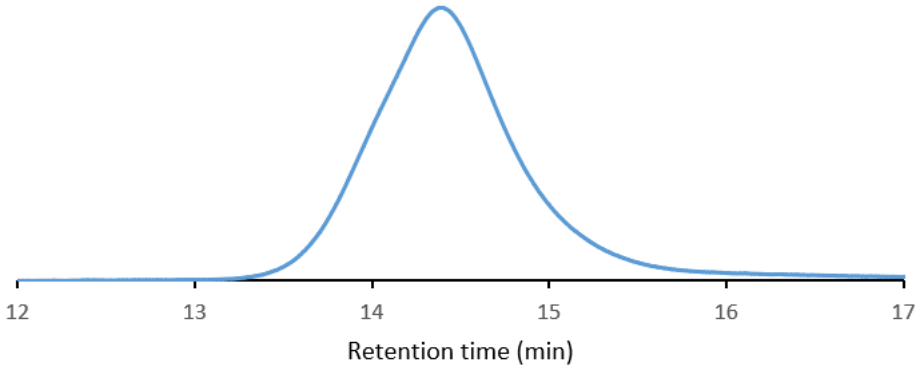

Figure S62 SEC trace of PLA (Table 1, entry 3)

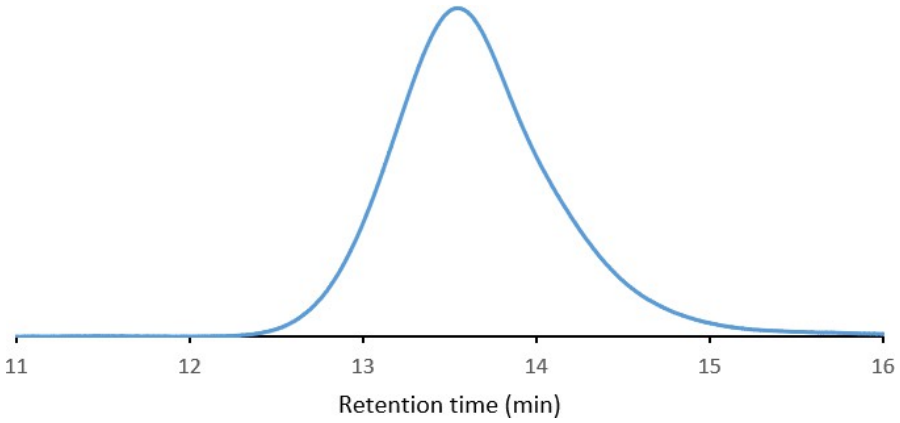

Figure S63 SEC trace of PLA (Table 1, entry 4)

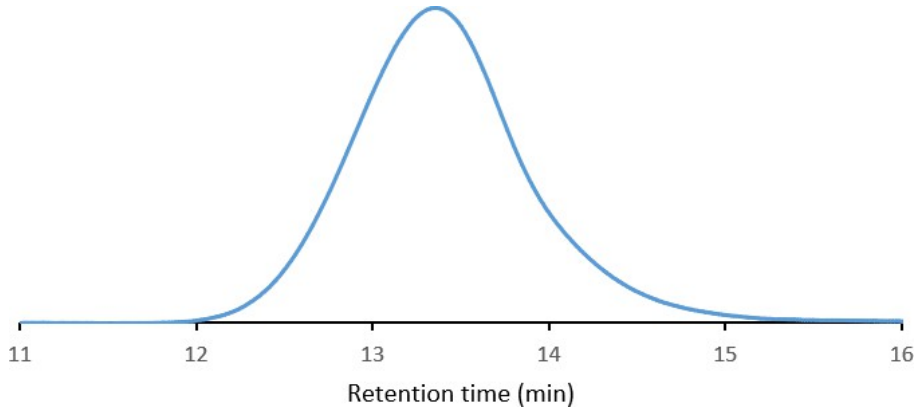

Figure S64 SEC trace of PLA (Table 1, entry 5)

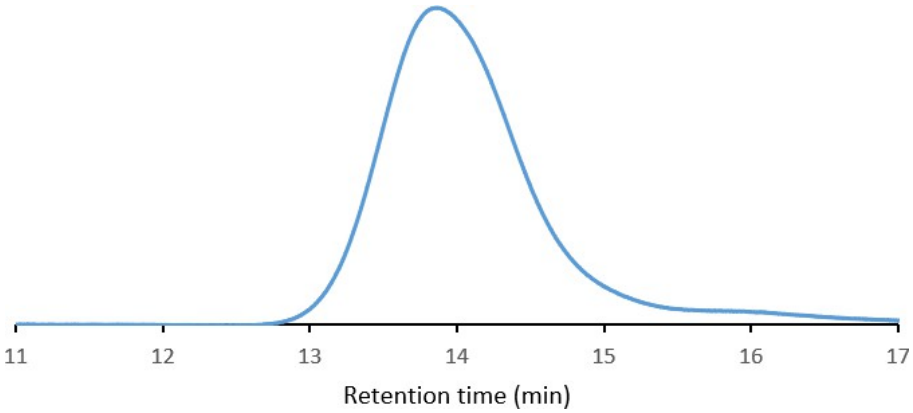

Figure S65 SEC trace of PLA (Table 1, entry 6)

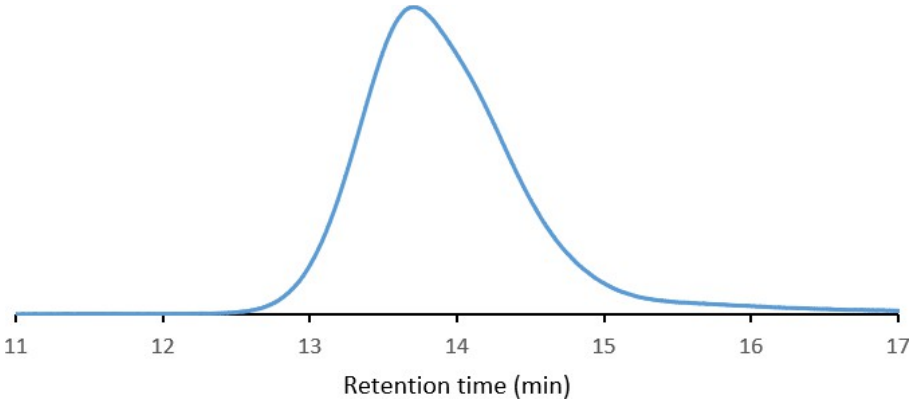

Figure S66 SEC trace of PLA (Table 1, entry 7)

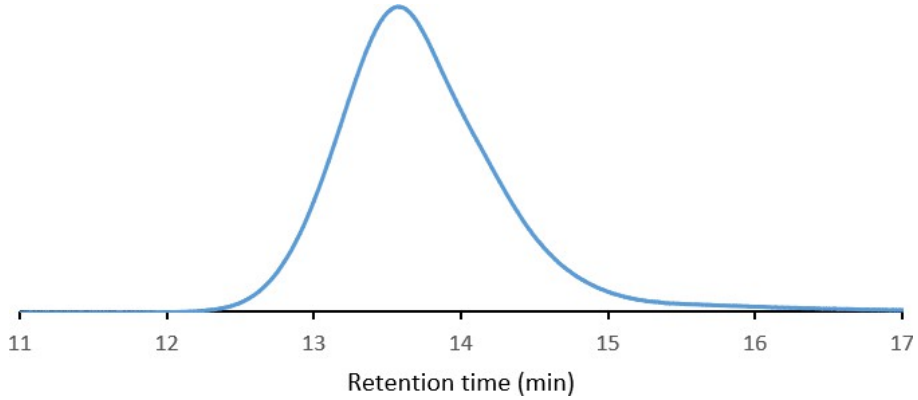

Figure S67 SEC trace of PLA (Table 1, entry 8)

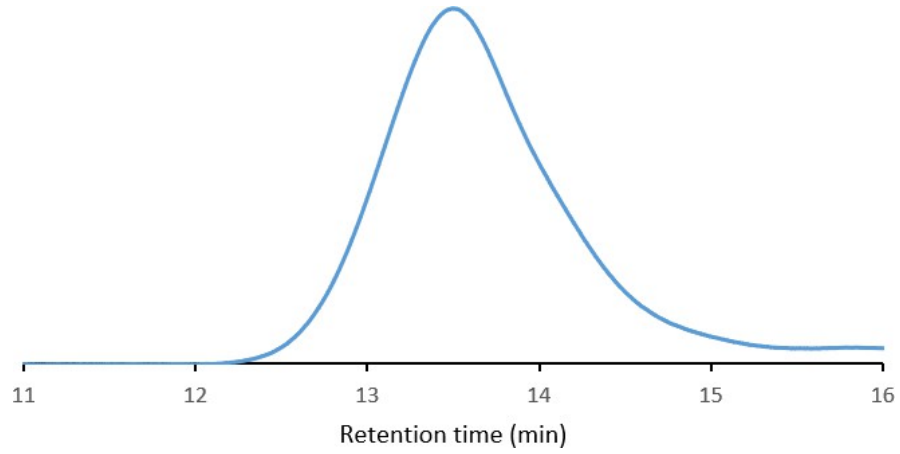

Figure S68 SEC trace of PLA (Table 1, entry 9)

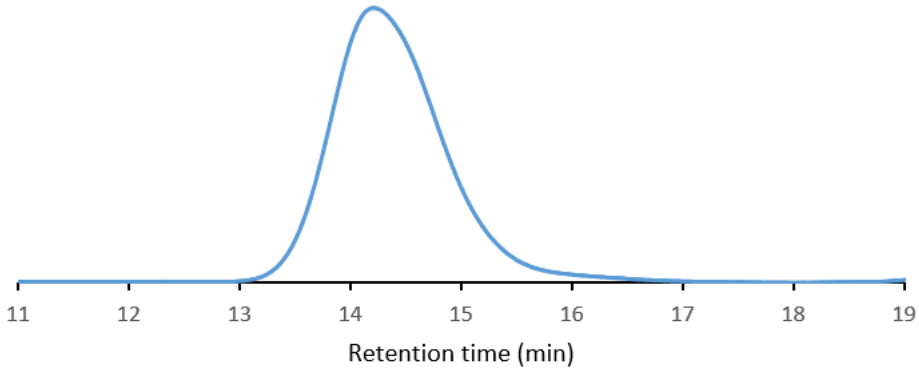

Figure S69 SEC trace of PLA (Table 1, entry 10)

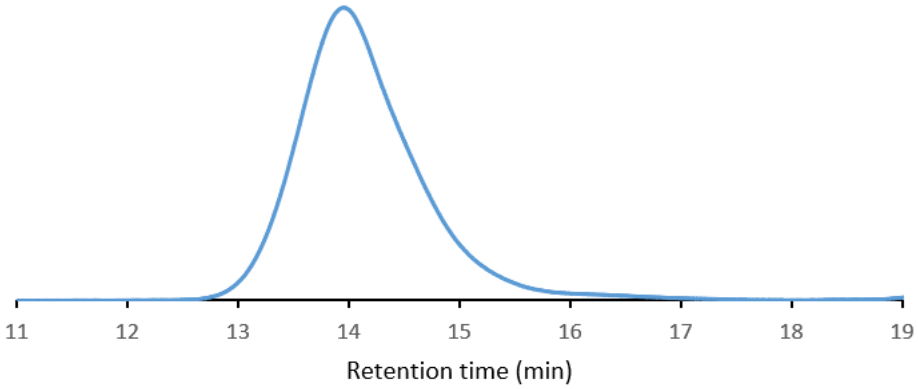

Figure S70 SEC trace of PLA (Table 1, entry 11)

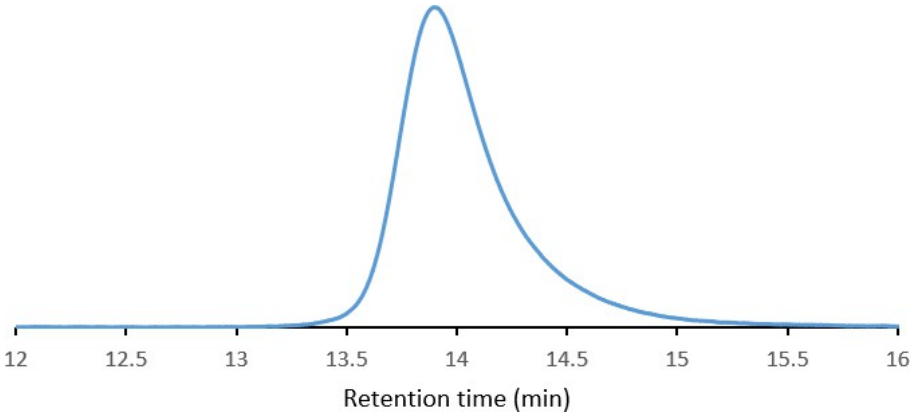

Figure S71 SEC trace of PLA (Table 2, entry 2)

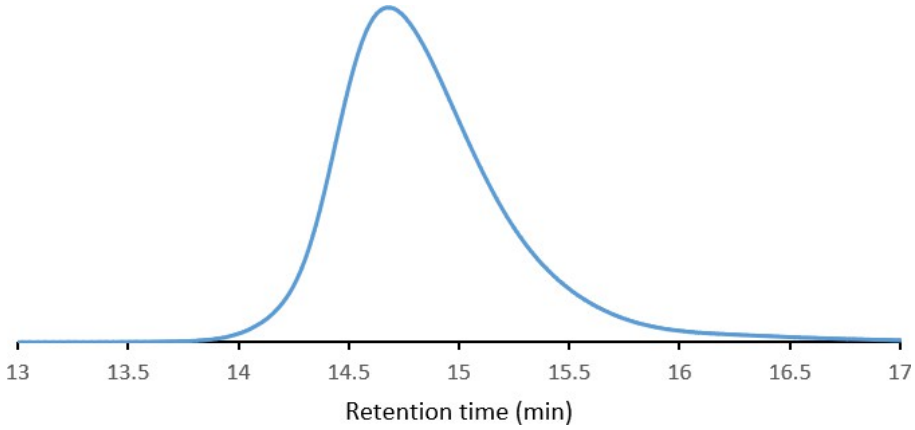

Figure S72 SEC trace of PLA (Table 2, entry 3)

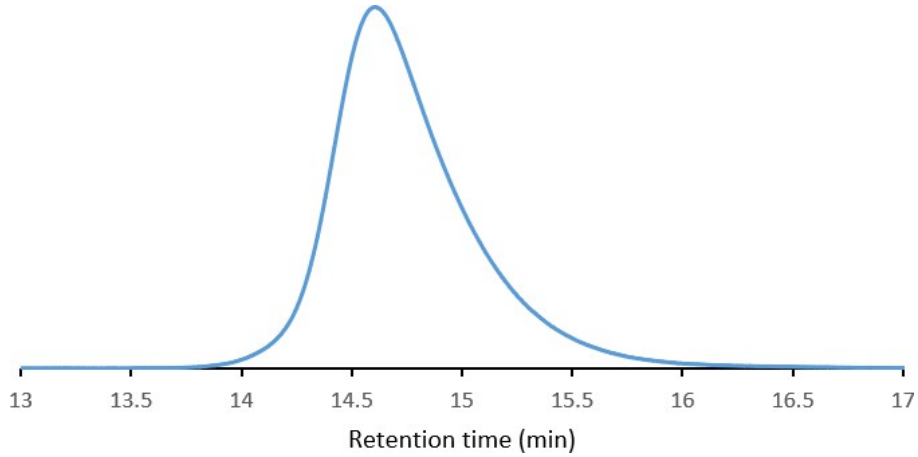

Figure S73 SEC trace of PLA (Table 2, entry 4)

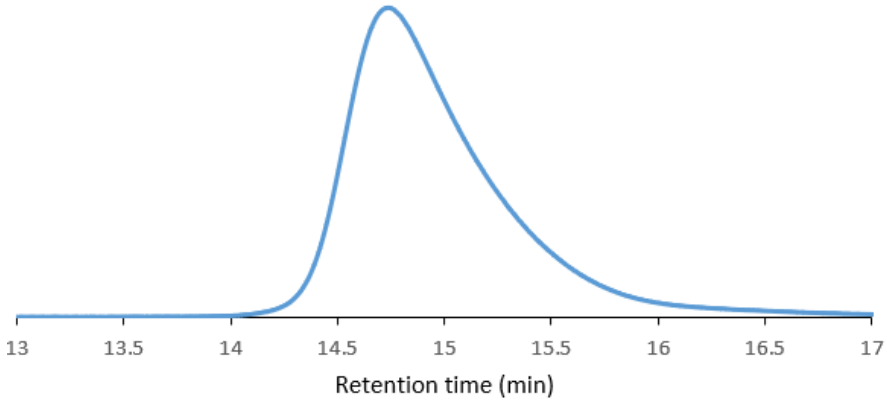

Figure S74 SEC trace of PLA (Table 2, entry 5)

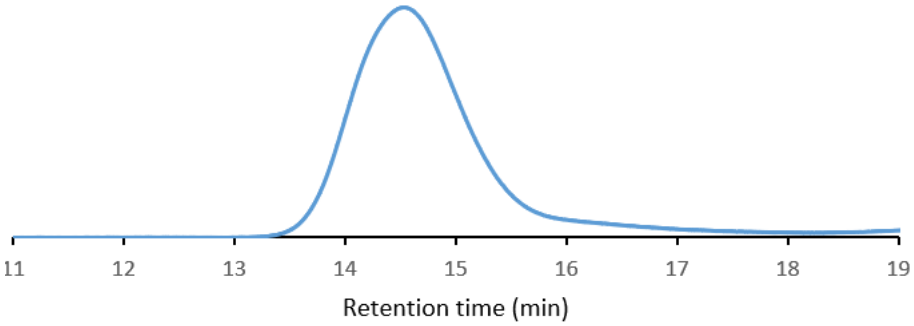

Figure S75 SEC trace of PLA (Table S6, entry 1)

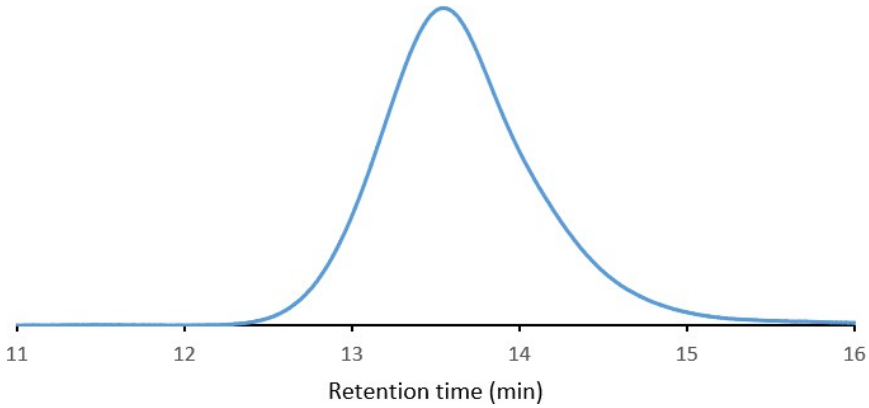

Figure S76 SEC trace of PLA (Table S6, entry 2)

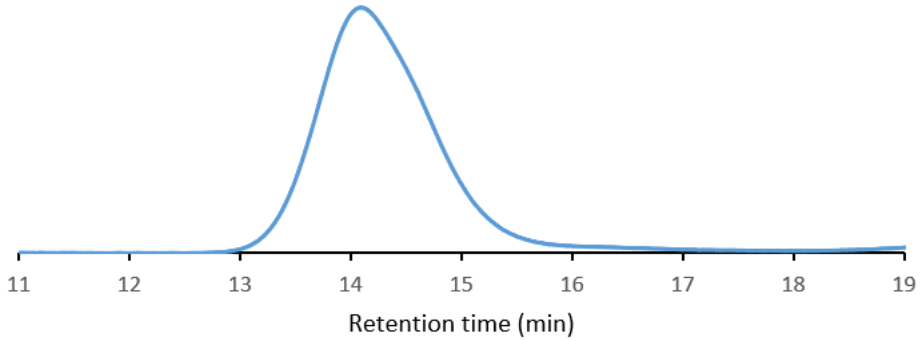

Figure S77 SEC trace of PLA (Table S6, entry 3)

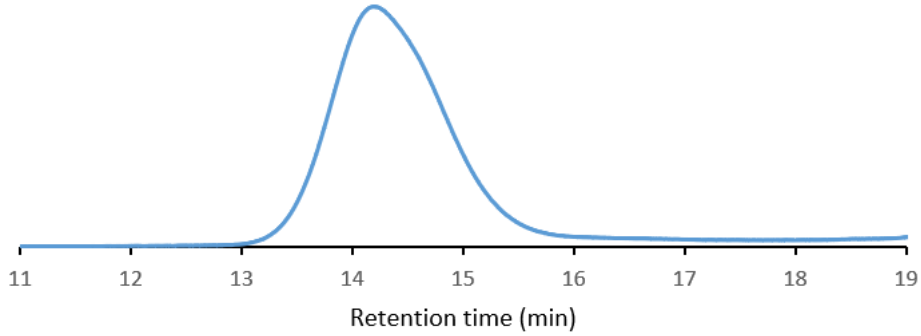

Figure S78 SEC trace of PLA (Table S6, entry 4)

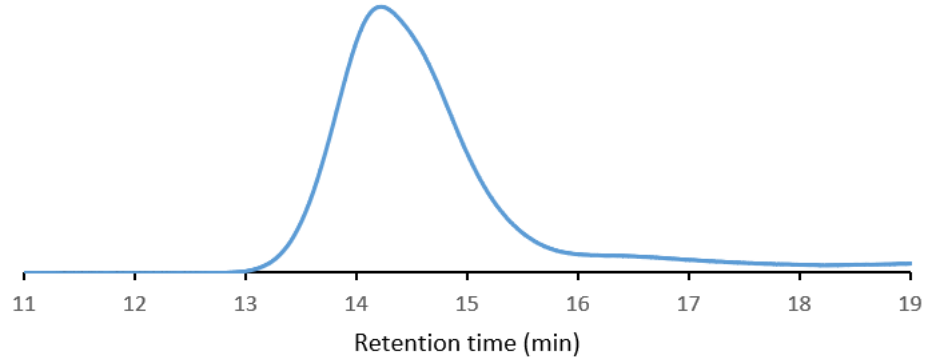

Figure S79 SEC trace of PLA (Table S6, entry 5)

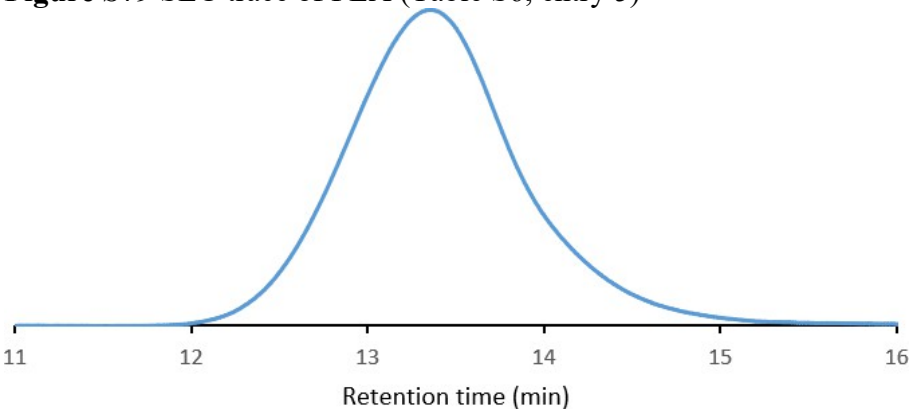

Figure S80 SEC trace of PLA (Table S6, entry 6)

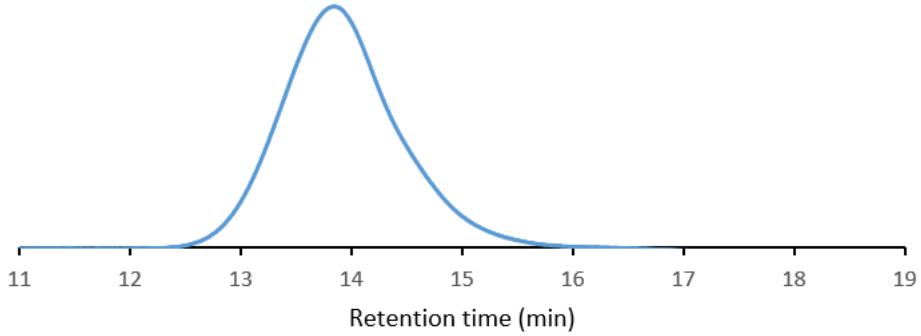

Figure S81 SEC trace of PLA (Table S6, entry 7)

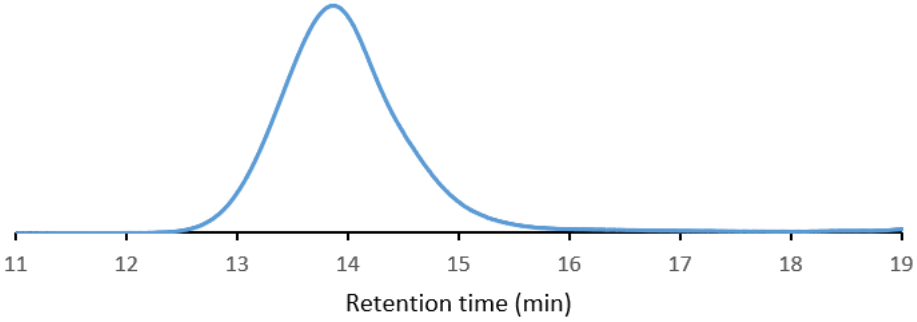

Figure S82 SEC trace of PLA (Table S6, entry 8)

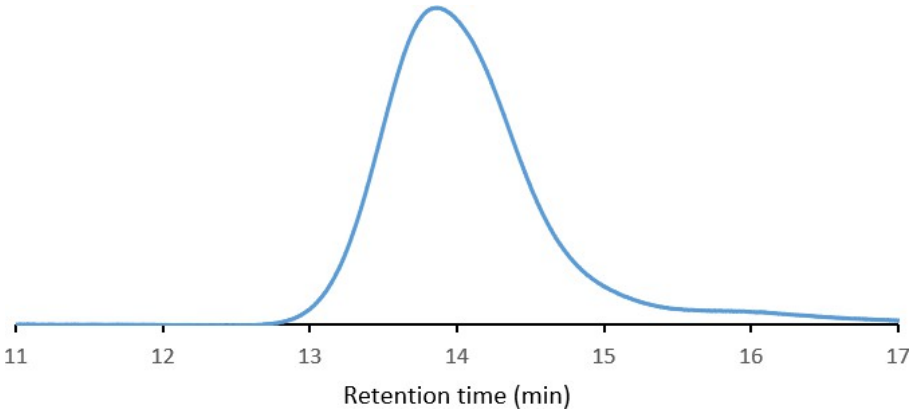

Figure S83 SEC trace of PLA (Table S6, entry 9)

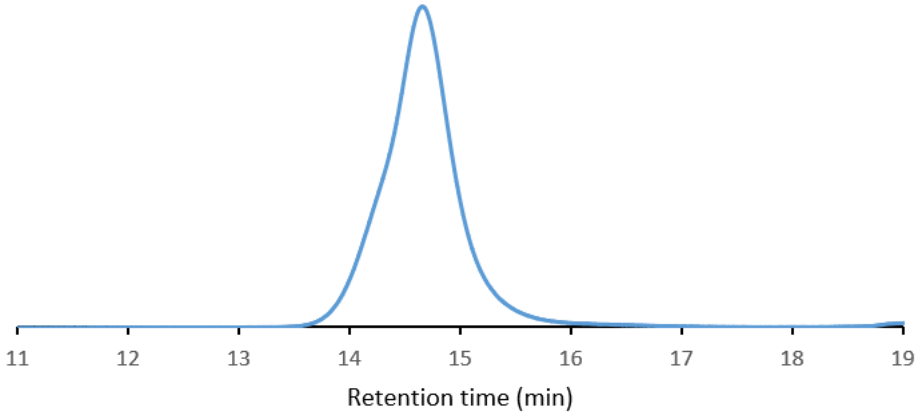

Figure S84 SEC trace of PLA (Table S6, entry 10)

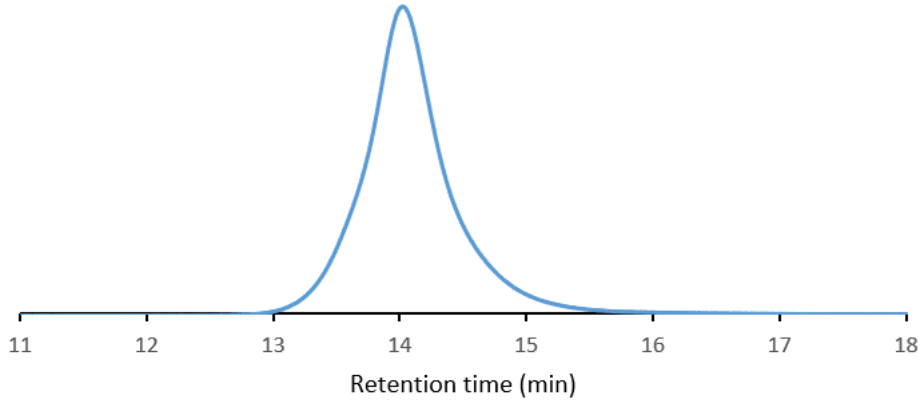

Figure S85 SEC trace of PLA (Table S6, entry 11)

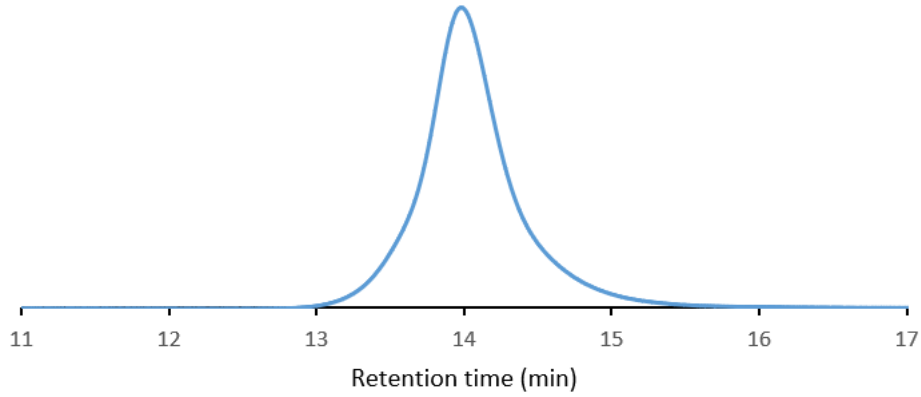

Figure S86 SEC trace of PLA (Table S6, entry 12)

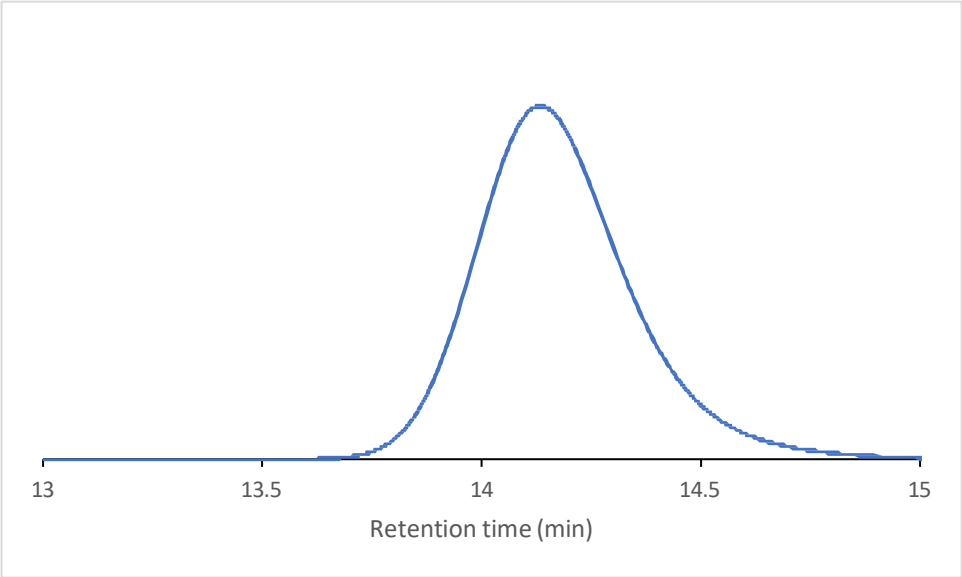

Figure S87 SEC trace poly(methyl methacrylate)standard (PMMA standard M_n = 55.9, $Đ$ = 1.03, determined M_n = 55.9, $Đ$ = 1.04)

F. References

1. O. T. Beachley and R. N. Rusinko, *Inorg. Chem.*, 1979, **18**, 1966-1968.
2. J. Bresien, A. Schulz, L. S. Szych, A. Villinger and R. Wustrack, *Dalton Trans.*, 2019, **48**, 11103-11111.
3. W. Gao and D. M. Cui, *J. Am. Chem. Soc.*, 2008, **130**, 4984-4991.
4. J. A. M. Vanbeek, G. Vankoten, G. Dekker, E. Wissing, M. C. Zoutberg and C. H. Stam, *J. Organomet. Chem.*, 1990, **394**, 659-678.
5. T. Ebrahimi, D. C. Aluthge, B. O. Patrick, S. G. Hatzikiriakos and P. Mehrkhodavandi, *ACS Catal.*, 2017, **7**, 6413-6418.